MOLECULAR AND CELLULAR CHARACTERIZATION OF THE CYP26B1-NULL LIMB PHENOTYPE

by

HELEN DRANSE

A thesis submitted in partial fulfillment of

the requirements for the degree of

MASTER OF SCIENCE

in

THE FACULTY OF GRADUATE STUDIES

(Cell and Developmental Biology)

THE UNIVERSITY OF BRITISH COLUMBIA

(Vancouver)

November 2010

ABSTRACT

Cyp26b1, a retinoic acid (RA)-metabolizing enzyme, is expressed in the developing limb bud and *Cyp26b1*$^{-/-}$ mice present with severe early limb defects characterized by truncated skeletal elements and oligodactyly. These malformations have previously been attributed to a patterning defect; however, recent reports suggest that RA is dispensable for limb patterning. In this study, we examined the role of endogenous retinoid signalling in skeletogenesis using *Cyp26b1*$^{-/-}$ mice and transgenic mice in which *Cyp26b1* is conditionally deleted under control of the *Prrx1* promoter beginning at ~E9.5 (*Prrx1Cre*$^{+}$*/Cyp26b1*$^{fl/fl}$). We found that the limb phenotype in *Prrx1Cre*$^{+}$*/Cyp26b1*$^{fl/fl}$ mice was less severe than *Cyp26b1*$^{-/-}$ animals and that a difference in retinoid signalling contributed to the difference in phenotypes. We systematically examined the role of RA signalling in chondrogenesis and found that *Cyp26b1*$^{-/-}$ cells are maintained at a pre-chondrogenic stage, exhibit reduced chondroblast differentiation, and exhibit a modest impact on chondrocyte hypertrophy. Furthermore, *Cyp26b1*$^{-/-}$ mesenchyme exhibited an increase in the expression of *Scleraxis* and other tendon markers, indicating that increased retinoid signalling in the limb maintains the ability of precursor cells to commit to other mesenchymal lineages. We conclude that RA signalling negatively impacts chondrogenesis before the onset of *Ihh* signalling, and has a positive impact on chondrocyte hypertrophy. This suggests that the limb phenotype in *Cyp26b1*$^{-/-}$ animals results from defects in the execution of a patterning program, and not so much in the patterning program itself.

PREFACE

A version of this thesis will be submitted for publication:

Dranse, H.J., Petkovich, M., and T.M. Underhill. Genetic deletion of *Cyp26b1* negatively impacts limb skeletogenesis by inhibiting chondrogenesis.

All of the following were carried out by Helen Dranse and Dr. T. Michael Underhill: identification and design of research program, performing the research, data analyses, and manuscript preparation.

Our collaborator, Dr. Martin Petkovich, was responsible for generating and providing the *ScxGFP*$^{+}$ and *Cyp26b1*$^{-/-}$ mice, respectively.

All animal work was approved by the UBC Animal Care Committee, Certificate #A07-0094.

TABLE OF CONTENTS

ABSTRACT ii

PREFACE iii

TABLE OF CONTENTS iv

LIST OF TABLES viii

LIST OF FIGURES ix

LIST OF ABBREVIATIONS x

ACKNOWLEDGEMENTS xii

CHAPTER 1: INTRODUCTION 1

Skeletal Development 1

Limb development 2

Endochondral ossification 3

Cellular commitment to chondrogenesis and condensation formation 4

Chondroblast differentiation 4

Prehypertrophy and hypertrophy 5

Chondrocyte terminal differentiation 6

Cartilage growth 6

Micromass culture 7

Mesenchymal cells and the chondrogenic and tendogenic lineages 7

Retinoid signalling 8

Retinoid action 9

Retinoid distribution 10

RA and limb development 11

A potential role for RA in the P-D patterning of the limb 12

Role of RA in chondrogenesis 14
Summary and objectives 15
CHAPTER 2: MATERIALS AND METHODS 23
Mice 23
Generation and maintenance of mouse strains 23
Genotyping 23
Reagents 24
Skeletal analysis 24
E18.5 embryos 24
E15.5 embryos 25
Establishment of primary mesenchymal cultures 25
Reporter-based assays 26
Plasmid constructs 26
Transfection of cultures 26
Analysis of reporter gene activity 26
Staining of micromass cultures 27
Peanut agglutinin (PNA) staining 27
Alcian blue staining 27
Immunofluorescence 27
RNA isolation 28
RNA isolation from primary cell cultures 28
RNA isolation from tissue 28
RT-qPCR 28
LacZ staining 29

Microscopy and image acquisition 29

Statistical analysis 30

CHAPTER 3: RESULTS 35

Prrx1Cre^{+}*/Cyp26b1*$^{-/-}$ mice exhibit limb malformations less severe than *Cyp26b1*$^{-/-}$ mice 35

Levels of retinoid signaling are increased in *Cyp26b1*$^{-/-}$ limb buds and to a lesser extent in *Prrx1Cre*$^{+}$*/Cyp26b1*$^{fl/fl}$ animals 36

Increased retinoid signalling negatively affects chondrogenesis 38

Cyp26b1$^{-/-}$ cells do not progress normally through the chondrogenic program 40

Cyp26b1$^{-/-}$ cells are maintained at a pre-chondrogenic stage 40

Cyp26b1$^{-/-}$ cells exhibit reduced chondroblast differentiation 41

Deletion of *Cyp26b1* has a modest impact on chondrocyte hypertrophy 41

The chondrogenic potential of proximal limb cells is more affected by changes in RA signalling 43

Increased expression of tendon markers in *Cyp26b1*$^{-/-}$ animals 44

CHAPTER 4: DISCUSSION 62

Regulation of chondrogenesis by RA 62

RA and chondrocyte hypertrophy 63

RA and multipotent mesenchymal cells - cell fate lineage decisions 65

CHAPTER 5: CONCLUSION 69

Discussion of goals 69

Significance of research 70

Developmental biology 71

Cell science 71

Strengths and limitations 71

Strengths 71

Limitations 72
Potential applications of research findings 72
Future research directions 73
REFERENCES 76
APPENDIX 85

LIST OF TABLES

Table 1. Generation of embryonic genotypes 31

Table 2. Genotyping parameters 32

Table 3. Primers and probes designed for RT-qPCR 33

LIST OF FIGURES

Figure 1. Mouse forelimb development 17

Figure 2. Overview of the chondrogenic program 19

Figure 3. Retinoid action 21

Figure 4. Limb malformations are less severe in *Prrx1Cre*$^{+/}$*Cyp26b1*$^{fl/fl}$ mice than *Cyp26b1*$^{-/-}$ mice 46

Figure 5. Retinoid signalling is increased in *Cyp26b1*$^{-/-}$ limbs and to a lesser extent in *Prrx1Cre*$^{+/}$*Cyp26b1*$^{fl/fl}$ limbs 48

Figure 6. Chondrogenesis decreases in response to elevated levels of RA signalling. 50

Figure 7. Cells from *Cyp26b1*$^{-/-}$ limb mesenchyme express/retain markers indicative of pre-cartilaginous condensations 52

Figure 8. Prechondrogenic cells from *Cyp26b1*$^{-/-}$ animals exhibit reduced differentiation. 54

Figure 9. *Cyp26b1*$^{-/-}$ cells exhibit little change in hypertrophy 56

Figure 10. Proximally-derived cells are more sensitive to changes in retinoid signalling. 58

Figure 11. Limb mesenchyme from *Cyp26b1*$^{-/-}$ exhibit increases in the expression of tendon markers 60

Figure 12. A model for the role of RA in regulating mesenchymal cell fate during limb development. 67

Figure A1. Additional analysis of *Cyp26b1* transgenic mice. 86

Figure A2. Changes in gene expression with ketoconazole treatment. 88

Figure A3. Ketoconazole and DEAB treatments. 90

Figure A4. Inhibition of chondrogenesis reflects an increase in tenogenesis. 92

LIST OF ABBREVIATIONS

ADH	Alcohol dehydrogenase
AER	Apical ectodermal ridge
ALDH	Aldehyde dehydrogenase
ALP	Alkaline phosphatase
BMP	Bone morphogenetic protein
CRABP	Cellular retinoic acid binding protein
CYP	Cytochrome P450
DEAB	Diethylaminobenzaldehyde
E	Embryonic day
EGFP	Enhanced green fluorescent protein
FD	Forelimb distal
FGF	Fibroblast growth factor
FL	Forelimb
FP	Forelimb proximal
HD	Hindlimb distal
HL	Hindlimb
HP	Hindlimb proximal
IHH	Indian hedgehog
LUC	Luciferase
P	Proximal
P-D	Proximo-distal
PCR	Polymerase chain reaction

PNA	Peanut agglutinin
PTHr	Parathyroid hormone-related protein receptor
PTHrP	Parathyroid hormone-related protein
q-PCR	Quantitative PCR
RA	Retinoic acid
RAR	Retinoic acid receptor
RARE	Retinoic acid response element
RLU	Relative light units
RXR	Retinoid X receptor
SHH	Sonic hedgehog
SOX	SRY-box containing
TGF	Transforming growth factor
WNT	Wingless
ZPA	Zone of polarizing activity

ACKNOWLEDGEMENTS

First and foremost, I would like to thank my supervisor, Michael Underhill, for giving me the opportunity to work in his lab and for all of the help and guidance he has given me over the past two years. I would also like to thank Fabio Rossi, Tim O'Connor, and Pamela Hoodless for taking the time to be on my committee and for their helpful insights.

A big thank you to all past and present members of the Underhill lab, especially Kerstin Boese, Matt Cowan, Erin Graham, Arthur Sampaio, Alex Scott, and Le Su, as well as many others at the BRC and UBC. I would also like to thank the Petkovich lab for getting me started on *Cyp26b1* and for their help over the years.

I am grateful for financial support from the Skeletal Regenerative Medicine Team, the Canadian Arthritis Network, and the Michael Smith Foundation for Health Research. Finally, special thanks to the Spears family, L.P., and M.M.

CHAPTER 1: INTRODUCTION

Skeletal Development

The musculoskeletal system is critical for providing structure, protection, and mobility to vertebrates and is comprised of a variety of tissues including muscle, bone, cartilage, tendon, and ligaments. The skeletal system, consisting of bone and cartilage, form from multipotent mesenchymal progenitor cells and involves both skeletal patterning to define the size and location of different skeletal elements, and the coordinated differentiation of skeletogenic cells. This occurs through two different processes - intramembranous ossification and endochondral ossification. The first, intramembranous ossification, involves the direct conversion of undifferentiated mesenchymal cells into bone, and elements such as bones of the face and the flat bones of the skull, form through this process. However, the majority of the vertebrate skeleton, including the appendicular and axial skeletons, the sternum, pelvis, components of the craniofacial skeleton, and the base of the skull, form through endochondral ossification. This is a process in which mesenchymal cells differentiate into chondrocytes and produce a cartilage template that is subsequently replaced by bone (Figure 1).

In addition to playing an essential role in skeletogenesis, cartilage is a permanent connective tissue that persists into adulthood in airways, joints, and ears, and the formation of cartilage growth plates constitutes the principal mechanism allowing longitudinal body growth (Olsen et al., 2000). However, despite the importance of cartilage in both embryonic development and adulthood, little is known about the underlying mechanisms regulating cartilage formation, or chondrogenesis. This project aims to study the molecular mechanisms that underlie the commitment and subsequent differentiation of mesenchymal cells to a chondrogenic fate, using the mouse limb as a developmental model.

Limb development

The vertebrate limb has been used for decades as a model system to investigate the mechanisms that control patterning and cell differentiation during embryogenesis. Limb development involves the morphogenesis of a complex, but systematically reproducible structure, and thus acts as framework to study the factors and cell interactions that regulate these processes. Phenotypic alterations provide an easy "read-out" and the limb can easily be accessed and manipulated for experimental purposes.

The murine limb originates as an outgrowth of mesenchyme, encased in ectoderm, that buds from the lateral plate of the embryo. Undifferentiated mesenchymal cells at the distal tip of the limb bud, in what is termed the "progress zone", give rise to most cell types of the mature limb, including the dermis, perichondrium, cartilage, bone, muscle connective tissue, tendons, and ligaments (Summerbell et al., 1973). Muscle and endothelial cells of the limb originate from a somitic precursor and migrate in to the limb bud during development (Tabin and Wolpert, 2007).

Several signalling centres coordinate the patterning and growth of the limb; these include the apical ectodermal ridge (AER) and the zone of polarizing activity (ZPA). The AER is a ridge of ectoderm along the distal edge of the limb bud that secretes fibroblast growth factor (FGF) signals and supports cell survival and outgrowth of the proximal-distal (P-D) axis, while the ZPA secretes SHH and is responsible for patterning the anterior-posterior axis (Saunders, 1948; Niswander et al., 1993; Riddle et al., 1993). Additionally, WNT-7a is secreted from the dorsal ectoderm, which patterns the dorsal-ventral axis (Parr and McMahon, 1995). The interplay between signals from the AER, ZPA, and dorsal ectoderm results in the formation of three skeletal segments – the stylopod (humerus or femur), the zeugopod (radius/ulna and tibia/fibula),

and the autopod (wrist/ankle and fingers/toes). There are two models for the patterning of limb segments – the progress zone model and the early specification model. The progress zone model proposes that cell fate is determined by the amount of time spent close to AER, while the early specification model suggests that various limb segments are specified early in limb development, and subsequent development involves expansion of these progenitor populations before differentiation (Tabin and Wolpert, 2007). For both models, limb outgrowth occurs in a P-D sequence, such that the limb segments close to the trunk (stylopod) are specified and differentiate earlier that those located far from it (autopod) (Saunders, 1948; Summerbell et al., 1973). The size and shape of developing skeletal elements relies on this spatio-temporal control of lineage-specific chondroblast differentiation, as it establishes a template for the bone primordia that will form through endochondral ossification (Underhill and Weston, 1998; Weston et al., 2003).

Endochondral ossification

Endochondral ossification provides the first structural template in the embryo and plays an important role in patterning the head, trunk, and limbs. As described above, the regulation of limb chondrogenesis involves a cascade of factors including members of the wingless (WNT), FGF, bone morphogenetic protein (BMP), sonic hedgehog (SHH), and retinoid signalling families that act together to specify the positional identity and fate of precursor cells and regulate their progression through the chondrogenic program (DeLise et al., 2000; Niswander, 2003; Barna and Niswander, 2007). This results in the appropriate spatio-temporal control of cell commitment to the chondrogenic lineage, condensation of mesenchyme, chondroblast differentiation, chondrocyte maturation, and replacement of cartilage by bone. Each step in this process is characterized by specific histological features, cellular activities, and gene expression profiles, which correspond to changes in cell morphology, proliferation, and extracellular matrix

production, and is controlled by a specific set of transcriptional activators, repressors, and associated factors (Figure 2).

Cellular commitment to chondrogenesis and condensation formation

The first step in endochondral ossification is the formation of cell mass condensations that prefigure the future skeletal elements, which is termed the "membranous skeleton". Mesenchymal cells migrate into the presumptive sites of limb formation from the lateral plate mesoderm (or from cranial neural crest of paraxial mesoderm for the head and trunk elements, respectively) and cells become tightly packed at these sites (Hall and Miyake, 2000). The process is mediated by a combination of pre-cartilage matrix and cell adhesion molecules, including N-Cadherin, N-CAM (*Ncam1*), Tenascin C (*Tnc*), Versican (*Vcan*), Hyaluronan, and fibronectin (DeLise et al., 2000; Lefebvre and Smits, 2005). Cell condensations can be visualised at the cellular level through peanut agglutinin (PNA) staining, as the PNA lectin binds to cell-surface expressed glycosylated proteins found on condensing mesenchymal cells (Hall and Miyake, 1992). The condensations establish the size and position of each nascent cartilage anlagen (Hall and Miyake, 2000). Commitment to a chondrogenic fate results in a decrease in the expression of *Runx2* and other lineage-specific factors, which are expressed in multipotent mesenchymal cells (Lefebvre and Smits, 2005). SRY-box containing (*Sox*) 9 is expressed in condensed mesenchyme and prechondrocytes, and plays an essential role in the commitment and differentiation of mesenchymal cells towards the chondrogenic lineage (Wright et al., 1995; Healy et al., 1996; Akiyama et al., 2002).

Chondroblast differentiation

The overt differentiation of prechondrocytes into fully committed and active chondrogenic cells is characterized by a switch from a fibroblast-like morphology to a spherical

cell shape and secretion of an abundant extracellular matrix ((Ede, 1983; Solursh, 1983). The cartilage matrix is a collagen-fibre network comprised primarily of type II collagen (*Col2a1*) and secondarily of type IX and XII. Additionally, Aggrecan (*Acan*), a very abundant proteoglycan in cartilage, forms large aggregates by binding to the glycosaminoglycan hyaluron, with the help of hyaluronan and proteoglycan link protein 1 (*Hapln1*). Other molecules present in cartilage include glycoproteins such as cartilage oligomeric protein (*Comp*), matrilin 1 (*Matn1*), chondroitin sulfate proteoglycan 4 (*Cspg4*), Melanoma inhibitory activity 1 (*Mia1*), and small proteoglycans including fibromodulin and perlecan (Ede, 1983; Solursh, 1983; Xie et al., 1999; de Crombrugghe et al., 2000; Okazaki and Sandell, 2004; Lefebvre and Smits, 2005). *Sox9* is highly expressed in addition to *L-Sox5* and *Sox6*, which are critical effectors of chondroblast differentiation, and are termed the "master chondrogenic trio" (Bell et al., 1997; Healy et al., 1999; Lefebvre, 2002; Ikeda et al., 2004). Chondroblast differentiation can be visualised at the cellular level by a reduction in PNA staining, as cells can no longer bind PNA after chondrogenic differentiation, and through visualisation of cartilage nodules with alcian blue stain, which binds to glycosaminoglycans in the extracellular matrix.

Prehypertrophy and hypertrophy

The cells in diaphyses of future long bones undergo prehypertrophy, and up-regulate extracellular matrix genes such as *Acan* and *Comp* and regulatory gene *Runx*2 (De Crombrugghe and Akiyama, 2009). A major phenotypic switch occurs as cells exit the cell cycle and increase in size. Subsequently, parathyroid hormone-related peptide receptor (*Pthr1*), Indian hedgehog (*Ihh*), and *Col10a1* are sequentially activated, which regulate chondrocyte maturation and hypertrophy. Patched (*Ptch)* expression is induced by and necessary for hedgehog signalling. (Colnot et al., 2005). When cells become hypertrophic, they stop expressing early cartilage

matrix genes, terminate *Pthr1* and *Ihh* expression, and up-regulate *Col10a1* and activate vascular endothelial growth factor (*Vegf*) (Lefebvre and Smits, 2005).

Chondrocyte terminal differentiation

As cells progress from hypertrophy to the terminal stage, they lose *Col10a1* expression and activate the expression of osteoblast-associated markers such as matrix metalloproteinase-13 (*Mmp13*), osteopontin (*Spp1*), and alkaline phosphatase (*Alp1*). The matrix around hypertrophic chondrocytes becomes mineralized, and cartilage becomes vascularized and osteoblasts are transported in by blood vessels (Colnot and Helms, 2001; Maes et al., 2010). The mineralized matrix serves as a template for deposition of trabecular bone, which is composed of a fibrillar network of collagen type I, II, and V, by incoming osteoblasts, and most of the chondrocytes will ultimately undergo apoptosis (Adams and Shapiro, 2002).

Cartilage growth

Cartilage growth involves two processes – interstitial growth and appositional growth. The first occurs through the unidirectional proliferation of chondrocytes, which results in parallel columns of dividing cells, an overall increase in internal cartilage mass, and longitudinal growth. However, with maturation, chondrocyte cellular turnover rate is very low, and the majority of cartilage growth occurs appositionally. This is a process in which new cartilage forms on the surface and is achieved through the action of chondrocytes that are derived from the perichondrium, which is a thin layer of mesenchymal cells on the periphery of endochondral skeletal elements and growth plate cartilage (Kronenberg et al., 2009). The perichondrium is a rich source of undifferentiated mesenchyme and has high levels of *Twist1* and *Fgf18* expression, which contribute to the maintenance of cells in a progenitor state (Hinoi et al., 2006; Reinhold et al., 2006).

Micromass culture

The chondrogenic process can be studied *in vitro* using the micromass culture system, in which primary limb mesenchyme (PLM) is dissociated into single cells and plated at a high density. The cells condense and form aggregates that differentiate into cartilage nodules, which accurately and reliably recapitulate the formation and maturation of cartilage during normal embryonic development (Ahrens et al., 1977). The sequence of gene expression in PLM cultures is similar to the chondrogenic differentiation process *in vivo*, and is useful for defining spatio-temporal differences in limb mesenchyme potential.

Mesenchymal cells and the chondrogenic and tenogenic lineages

In the limb, chondrocytes are formed from mesenchymal progenitor cells that are derived from the lateral plate mesoderm. These multi-potent cells have the ability to differentiate into several mesodermal lineages including bone, cartilage, tendon, marrow stroma, and fat (Pearse et al., 2007). There is some overlap between the early molecular mechanisms that underlie lineage-specific differentiation, and in particular, a close association between chondrogenesis and tenogenesis exists.

During embryonic limb development, mesenchymal condensations express *Sox9*, *Scx*, and *Runx2*. A temporal and spatial relationship between *Sox9* and *Scx* exists in which *Sox9* and *Scx* expression ultimately become restricted to skeletal primordia and tendon, respectively (Asou et al., 2002; Akiyama et al., 2005). Cell fate determination occurs at the condensation stage, and commitment of multi or bi-potent progenitor cells to a chondrogenic lineage results in a decrease in *Scx* expression, while commitment to a tenocyte fate results in a decrease in *Sox9* (Soeda et al., 2010). The differentiated cells have a molecular and cellular phenotype that is characteristic to their function; chondrocytes express *Col2a1* and *Acan*, and are round, while tenocytes express

Tenomodulin (*Tnmd*), Type I collagen (*Col1a1*), Mohawk (*Mkx*), *Eya2*, and *Tgfb2*, and exhibit an elongated fusiform shape (Xu et al., 1997; Docheva et al., 2005; Pryce et al., 2009; Ito et al., 2010). Similar to chondrogenic differentiation, tenocyte differentiation occurs in a proximal-distal direction that follows the outgrowth of the limb bud (Schweitzer et al., 2001), and is directed by growth factors and signalling molecules. Importantly, changes in both the duration and nature of the signal that direct mesenchymal cells to specific lineages can affect tissue morphogenesis. A signalling molecule that is known to play an important role in regulating cell differentiation is retinoic acid (RA), and the focus of this research is the role of RA in skeletal development and the lineage-specific differentiation of mesenchymal cells.

Retinoid signalling

It has been known for years that vitamin A and its derivatives, the retinoids, play fundamental roles in the development and homeostasis of many different tissues and organ systems. Early rodent studies shown that vitamin A, or retinol, is important in embryonic development as females maintained in a vitamin A deficient state had increased rates of reproductive failure and embryos exhibited a spectrum of embryonic malformations. Treatment with retinoic acid (RA), was able to reverse the abnormalities, indicating that RA is the active metabolite (Pennimpede et al., 2010a). While animal models have shown that RA is indispensable for embryogenesis and organogenesis, intake of excess RA during pregnancy has also been shown to have teratogenic effects resulting in congenital malformations (Kalter and Warkany, 1961; Lammer et al., 1985; Ross et al., 2000). These studies have demonstrated that RA signalling is involved in the regulation of a wide range of developmental processes including neurogenesis, cardiogenesis, body axis extension, and skeletal, foregut, lung, pancreas, eye, and genitourinary tract development (Duester, 2008).

Retinoid action

In mammals, vitamin A is obtained from the diet or from maternal sources, and undergoes a series of enzymatic reactions to form its biologically active metabolite, RA. RA is a small lipophilic molecule that is typically associated with intracellular binding proteins such as cellular retinoic acid binding protein 2 (*Crabp2*) which is important for both sequestration and transportation of RA to nuclear receptors of the steroid receptor superfamily (Sessler and Noy, 2005). RA forms nuclear hormone complexes consisting of retinoic acid receptor (RAR) and retinoid X receptor (RXR) heterodimers (Mark et al., 2006; Niederreither and Dolle, 2008; Mark et al., 2009). In the absence of ligand, RAR-RXR heterodimers bind to retinoic acid response elements (RAREs) and recruit co-repressors, which mediate negative transcriptional effects by recruiting histone deacetylases and methyltransferase complexes, which stabilize the nucleosome structure so that DNA becomes largely inaccessible for transcription. Binding of RA leads to a conformational change of the RAR ligand-binding domain, release of co-repressors, and recruitment of co-activators (Germain et al., 2006). Through this method of ligand activation, the RARs directly control the transcriptional activity of target genes, and hundreds of genes are RA-inducible, either directly or through indirect cascades (Figure 3).

Both RARs and RXRs are encoded by three different isoforms – alpha, beta, and gamma. All receptor isoforms are widely expressed throughout the embryo during all stages of development, and while there is some tissue specificity for isoforms, targeted disruption of the RAR genes has shown that they exhibit considerable functional redundancy (Mark et al., 2009). This indicates that while RARs mediate RA signalling, any single receptor does not play a large role in the regulation of RA signalling. However, because the concentration of RA must be within a narrow range to avoid both deficiency and toxicity, the proper distribution of RA, and

thus RAR-mediated signalling, must be tightly controlled during embryonic development. This occurs through the coordinated expression of RA-synthetic and RA-catabolic enzymes.

Retinoid distribution

A reversible reaction catalyzed by retinol-specific alcohol dehydrogenases converts retinol to retinal, and RA is synthesized by a family of retinaldehyde dehydrogenases (ALDH1A1-3) that irreversibly oxidize retinal to form RA. In the developing embryo, regions that express *Aldh1a* genes generally correspond to regions that are rich in RA. *Aldh1a1*, *2*, and *3* are expressed in restricted temporal-spatial domains throughout embryogenesis, and ALDH1A2 is the most important of the three, being responsible for nearly all of the RA produced in the early embryo (Niederreither et al., 1999; Niederreither et al., 2000; Niederreither et al., 2001). A deficiency of *Aldh1a2* affects many developing systems including the forebrain, hindbrain, heart, limbs, and somites (Niederreither et al., 1999). These defects indicate that RA synthesis is required for embryonic patterning and/or development.

The degradation of RA is mediated by the action of Cytochrome P450 family members CYP26A1, B1, and C1, which hydroxylate RA to more polar molecules such as 4-hydroxy-RA, 18-hydroxy-RA, and 4-oxo-RA (White et al., 1996; Fujii et al., 1997; Ray et al., 1997). These products do not function as RAR ligands, and are more soluble which facilitates the excretion of RA from the organism. Each CYP26 enzyme exhibits a spatially distinct expression domain during development, with *Cyp26a1* being expressed in the tailbud and cervical mesenchyme, *Cyp26b1* in the hindbrain, limb buds, branchial arches, and craniofacial structures, and *Cyp26c1* in the hindbrain (MacLean et al., 2001; Abu-Abed et al., 2002; Tahayato et al., 2003). Targeted disruption of *Cyp26a1* and *Cyp26b1* lead to developmental abnormalities that phenocopy the teratogenic effects of RA. *Cyp26a1* knockout mice exhibit hindbrain patterning defects and

caudal regression (Abu-Abed et al., 2001), while *Cyp26b1* null mice have a number of defects including truncated limbs, malformed craniofacial structures, and hypoplastic testes (Yashiro et al., 2004; MacLean et al., 2007; Maclean et al., 2009). A loss of *Cyp26c1* does not appear to have any effect on embryonic development, but when lost in conjunction with *Cyp26a1* expression, results in a severe phenotype with embryos exhibiting anterior truncation of the brain (Uehara et al., 2007). These defects occur because regions where CYP26 enzymes are expressed are normally devoid of RA.

The coordinated expression of ALDH and CYP26 enzymes influences where RA signalling is able to occur in the developing embryo, and correlates with the dynamics of RA signalling. Regions of activated retinoid signalling can be visualised using mice that express an RA-responsive transgene, with the caveat that the reporter may not respond to very low levels of retinoid activity or reflect all regions of activated RA signalling (Rossant et al., 1991). Misregulation of RA signalling leads to a wide spectrum of defects as described above, and one such tissue that is exquisitely sensitive to changes in RA availability is the developing limb.

RA and limb development

RA has long been implicated in skeletal development as pregnant mice maintained on a vitamin A deficient diet or administered teratological doses of RA resulted in offspring with skeletal defects (Kwasigroch and Kochhar, 1980; Niederreither and Dolle, 2008). Targeted disruption of the RAR isoforms and ALDH/CYP enzymes, alone or in combination, have revealed roles for each of these proteins in controlling RA signalling and skeletal development. *Aldh1a2* deficient mice lack limb buds, while genetic inactivation of different combinations of *RARa, b, or g,* leads to alterations in the axial skeleton, craniofacial skeleton, and limbs (Lohnes et al., 1994; Dupe et al., 1999; Niederreither and Dolle, 2008). Furthermore, *Cyp26a1* knockout

mice have axial skeleton defects, and *Cyp26b1* knockout mice present with severe early limb defects characterized by a truncation of skeletal elements and hypodactyly (Abu-Abed et al., 2001; Yashiro et al., 2004).

In the developing limb, RA is produced locally by ALDH1A2 in the trunk mesoderm that lies proximal to the limb, but not in the limb bud itself between E9.5 and E10.5 (Niederreither et al., 1999; Mic et al., 2002; Gibert et al., 2006). High levels of RA metabolism occur through the action of CYP26B1, which is expressed in the distal portion of the newly formed limb bud. As the limb bud grows, *Cyp26b1* increases in intensity but remains restricted to the distal region (MacLean et al., 2001; Abu-Abed et al., 2002). *Cyp26b1* mRNA is abundant in the ectoderm, but excluded from the AER, and the specific sites of RA synthesis and degradation results in a graded distribution of RA which decreased P-D throughout the limb bud (Mic et al., 2004). This gradient of RA can be visualised using RARE-LacZ transgene-expressing reporter mice (Rossant et al., 1991), and has been hypothesized to play a role in the patterning of the P-D axis in the developing limb bud.

A potential role for RA in the P-D patterning of the limb

Over three decades of work exists that investigates the role of RA signalling in the instruction of limb bud patterning and development. Studies have shown that RA "proximalizes" the distal blastema of regenerating newt and axolotl limbs, and the extent of proximalization in regenerating limbs increases with the dose of RA (Maden, 1982; Crawford and Stocum, 1988; Brockes, 1997). Furthermore, local administration of synthetic molecules acting as RAR antagonists severely limited limb outgrowth in chick limbs (Helms et al., 1996; Stratford et al., 1996), and the limb defects present in *Cyp26b1* null mice have been attributed to a disruption or shortening of the P-D axis. In these mice, an expansion of proximal *Meis* genes and a down-

regulation of distal *Hox* genes, both of which are known to regulate limb patterning, is observed (Mercader et al., 2000; Yashiro et al., 2004). Altogether, these studies implicate that RA is playing an instructive role during limb bud patterning by acting as a "proximalizing" morphogenetic factor to active transcription of target genes and provide positional information to developing limb cells.

Recent reports, however, have argued that RA does not play an instructive role in limb patterning, but instead acts entirely permissively. An *Aldh1a2/3* double knockout that lacks all endogenous RA in the trunk exhibits normal hindlimb development, indicating that RA synthesis is dispensable for limb patterning and development, and is only essential to antagonize early axial FGF signals that would otherwise inhibit induction of the forelimb field (Lewandoski and Mackem, 2009; Zhao et al., 2009). Furthermore, disruption of all isotypes of *Rarg* in the *Cyp26b1* null background rescues the stylopod and some digit formation, while still exhibiting altered P-D gene expression similar to the *Cyp26b1* knockout (Pennimpede et al., 2010b). These results allow for the re-interpretation that *Cyp26b1* does not act to create a RA gradient across the limb, but rather to eliminate an RA signal from the body axis that would otherwise cause distal RA-induced limb teratogenesis. In other words, there is no clear evidence that a proximal RA signalling centre is required to establish the P-D axis, and that while excess RA can induce limb P-D defects, this may be an effect of increased and inappropriate RA exposure (pharmaceutical effects) rather than a natural, physiological role for RA in limb development. The more likely scenario is that endogenous RA signalling regulates cell differentiation and that inappropriate activation of this pathway inhibits differentiation and results in truncated limbs. Data from the RAR double knockouts are certainly consistent with this premise, in that, loss of *Rara* and *Rarg* leads to ectopic cartilage formation within the interdigital region. Interestingly,

these animals also present with heterotopic cartilages at a number of other anatomical sites, indicating that retinoid signalling may play a more general role in regulating the expression of the chondrogenic phenotype.

In order to address the role of RA in limb patterning and development, it is necessary to understand the role of retinoid action in the formation of developing skeletal elements.

Role of RA in chondrogenesis

As discussed, it has been known for years that both a deficiency and an excess of RA during embryogenesis results in skeletal abnormalities. In the case of RA teratogenecity, the severity of skeletal defects depends on both the timing and dose of RA, with skeletal malformations being most severe when RA is applied during the early stages of cartilage development (Shenefelt, 1972). This indicates that this time period in chondrogenesis is most sensitive to retinoid signalling.

Analysis of gene expression patterns in PLM cultures shows a dynamic expression of *Aldh1a2* and *Cyp26a1*. *Aldh1a2* is expressed during mesenchyme condensation and increases in plated cultures for 24 hours before peaking, while the onset of *Cyp26a1* expression occurs 12 hours later, but peaks at the same time as *Aldh1a2*. The expression profile of *Rarb*, a direct RAR-target gene, follows this same trend, indicating that their up-regulation is in response to RA signalling (unpublished data, TMU). This data demonstrates a transient increase in RA within the precartilaginous condensations, followed by a decrease in RA availability that is concordant with the onset of differentiation. Interfering with this "pulse" of RA signal leads to substantial changes in chondrogenesis, with sustained activation resulting in a reduction of chondroblast markers and inhibition of differentiation. Notably, a dose-dependent decrease in SOX9 reporter activity is observed with increasing doses of RA treatment. Conversely, antagonism of RA

signalling results in an increase in *Sox9* expression and earlier chondroblast differentiation (Weston et al., 2000; Weston et al., 2002). However, smaller nodules form because cells differentiate prematurely in the condensations (unpublished data, TMU). Altogether, this demonstrates a requirement for RAR-mediated repression for chondroblast differentiation to occur, and that RA regulates skeletal development partly by its control over timing of differentiation.

In addition to its inhibitory effect on chondroblast differentiation, RA has been shown to regulate later stages of chondrogenesis by decreasing *Sox9* expression to promote chondrocyte maturation and that RAR-mediated repression is necessary for *Acan* expression (Koyama et al., 1999; Williams et al., 2009; Williams et al., 2010). Consistent with this, very little RA signalling is found in the upper resting/proliferating region of the growth plate, but retinoid activity is observed in the lower growth plate, where maturation and hypertrophy occurs (Williams et al., 2010). By switching from RAR-mediated repression in early stages, to control the timing of condensation and chondroblast differentiation, to RAR-mediated activation at later stages, to coordinate the maturation of chondrocytes and replacement by bone, RA functions to precisely control the step-wise progression of cells through chondrogenesis.

Summary and objectives

Much of the skeleton, including the limb, forms through endochondral ossification. The precise spatio-temporal control of chondrocyte differentiation from multi-potential mesenchymal cells is required for the proper size and shape of developing skeletal elements and RA signalling has been shown to play an important role in regulating the step-wise progression of cells through different stages of chondrogenesis. While RA signalling has previously been thought to play a role in the P-D patterning of the developing limb, new evidence exists that RA is dispensable for

limb patterning. This project aims to re-address the role of RA in cartilage formation and limb development, using the *Cyp26b1* knockout mouse as a model. We hypothesize that the limb defects present in *Cyp26b1*-null mice are due to a defect in the execution of a patterning program and the objectives of this thesis include:

1. Generate and characterize a transgenic mouse with delayed deletion of *Cyp26b1*
2. Investigate the effect of increased endogenous RA signalling *in vivo* on different stages of the chondrogenic program
3. Determine the mechanism by which increased levels of RA affect cartilage formation *in vivo*

Figure 1. Mouse forelimb development

Mouse forelimb development begins at embryonic day (E) 9.5 with the formation of cell mass condensations that prefigure the future skeletal elements (light blue). Condensed cells differentiate into chondrocytes and produce an abundant extracellular matrix (dark blue). This matrix is subsequently mineralized and acts as a template for deposition of bone (red). Limb outgrowth occurs in a proximal-distal sequence such that elements closest to the trunk are specified and formed first. Hindlimb development follows that of forelimb development by ~0.5 days. Modified from (Weston et al., 2003).

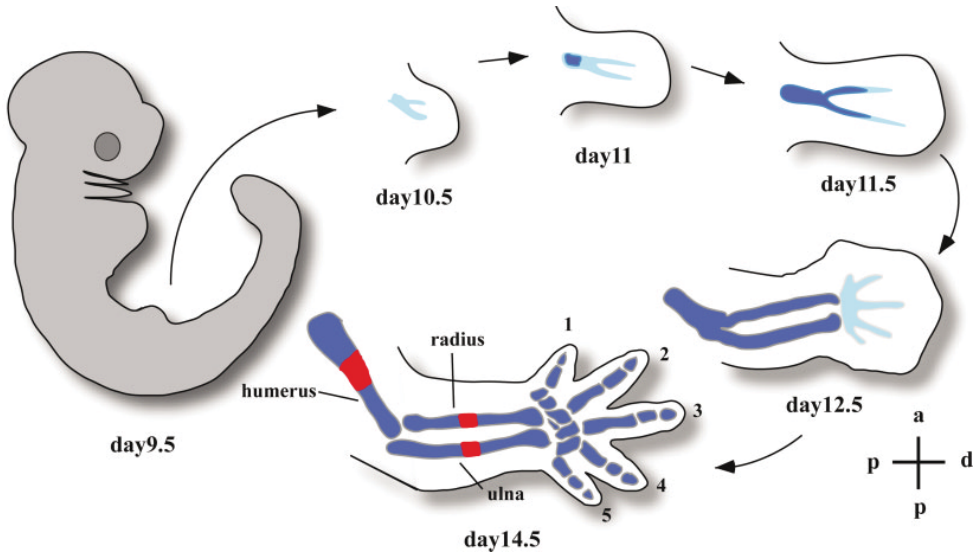
day9.5
day10.5
day11
day11.5
day12.5
day14.5
humerus
radius
ulna
1
2
3
4
5
a
p
d
p

Figure 2. Overview of the chondrogenic program

Mesenchymal progenitor cells are committed to the chondrogenic lineage and form cell mass condensations. Upon formation of precartilaginous condensations, cells overtly differentiate into chondroblasts which secrete an abundant extracellular matrix. As chondrocytes mature, they exit the cell cycle, increase in size, become pre-hypertrophic and then hypertrophic, and acquire the ability to mineralize their extracellular matrix, and ultimately undergo apoptosis. Each step of the chondrogenic program is characterized by a specific gene expression profile as indicated.

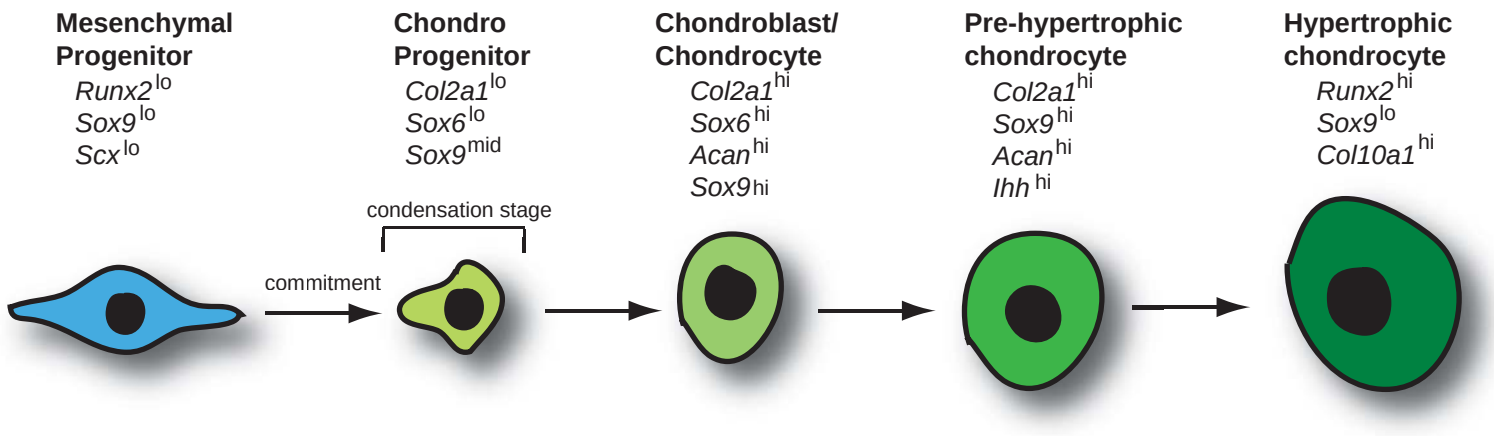
Mesenchymal Progenitor
Runx2lo
Sox9lo
Scxlo
Chondro Progenitor
Col2a1lo
Sox6lo
Sox9mid
condensation stage
commitment
Chondroblast/ Chondrocyte
Col2a1hi
Sox6hi
Acanhi
Sox9hi
Pre-hypertrophic chondrocyte
Col2a1hi
Sox9hi
Acanhi
Ihhhi
Hypertrophic chondrocyte
Runx2hi
Sox9lo
Col10a1hi

Figure 3. Retinoid action

In mammals, vitamin A (retinol) is obtained from the diet and a reversible reaction catalyzed by retinol-specific alcohol dehydrogenases (ADH) converts retinol to retinal. A family of retinaldehyde dehydrogenases (ALDH1A1-3) irreversibly oxidize retinal to form RA, which activates the transcription of hundreds of target genes involved in a variety of cellular processes. RA is degraded by cytochrome P450 enzymes (CYP26A1, B1, and C1) into inactive metabolites that are eliminated from the organism.

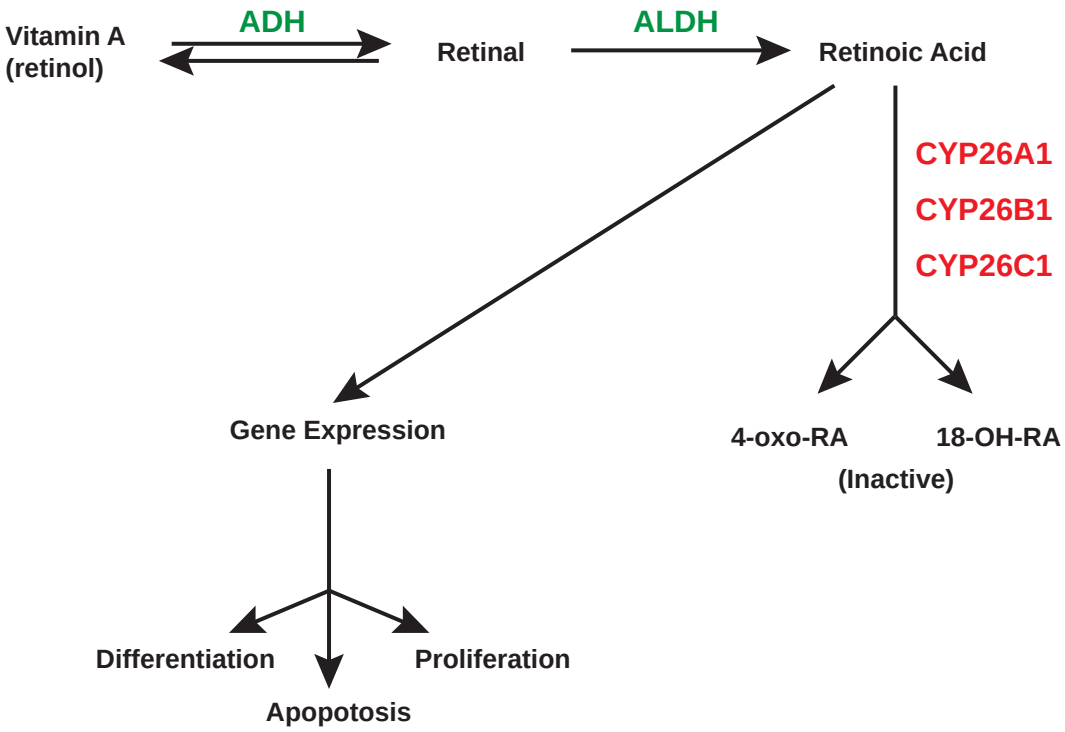
Vitamin A
(retinol)
ADH
Retinal
ALDH
Retinoic Acid
CYP26A1
CYP26B1
CYP26C1
Gene Expression
4-oxo-RA
18-OH-RA
(Inactive)
Differentiation
Proliferation
Apopotosis

CHAPTER 2: MATERIALS AND METHODS

Mice

Generation and maintenance of mouse strains

Cyp26b1$^{+/-}$ and *Cyp26b1*$^{fl/fl}$ mice were obtained from Dr. Martin Petkovich (Queen's University, Kingston, ON) and *ScxGFP*$^{+}$ mice were obtained from Dr. Ronen Schweitzer (Portland Shriners Research Center, Portland, OR). *RARE-LacZ* and *Prrx1Cre*$^{+}$ mice were obtained from Jackson Laboratory (Bar Harbor, ME, USA). The mice used in the studies described were of a mixed genetic background and timed matings were established by housing females with males overnight and checking females daily for vaginal plugs. Noon of the day that a plug appeared was denoted as embryonic day (E) 0.5, and on the appropriate day, pregnant females were humanely euthanized and embryos collected. Embryonic genotypes were generated as shown in Table 1. Importantly, some germline recombination has been observed to occur in the offspring of female *Prrx1Cre*$^{+}$ expressing mice (Logan 2002), so only male Cre^{+} mice were used in these experiments. Animals were maintained in a facility at the Biomedical Research Centre (UBC) and experimental protocols were conducted in accordance with approved and ethical treatment standards of the University of British Columbia.

Genotyping

Ear punches (adult mice) or yolk sac tissue (embryos) were collected and digested in proteinase K buffer (50mM Tris pH8.0, 2mM NaCl, 10mM EDTA, 1% SDS, 1 mg/ml proteinase K) at 55°C for 40 minutes. Samples were then boiled at 95°C for 10 minutes and subsequently genotyped using standard PCR conditions (10X PCR buffer (200mM Tris-HCl, pH 8.4, 500mM KCl), 1.5mM $MgCl_2$, 0.4µM of primer 1 and 0.2µM of primer2/3 or forward/reverse primers,

0.2mM dNTP, and Taq Polymerase (Invitrogen)). Primer sequences, PCR conditions, and amplicon sizes for genotyping of *Cyp26b1*, *RARE-LacZ*, *Cre*$^{+}$, and *GFP*$^{+}$ transgenic mice are shown in Table 2. Products were run on a 2% agarose gel and visualized using AlphaImager (Alpha Innotech) using AlphaEaseFC software. *ScxGFP*$^{+}$ embryos were also genotyped by visualization of GFP expression with fluorescence microscopy.

Reagents

Ketoconazole and diethylaminobenzaldehyde (DEAB) were obtained from Sigma Aldrich, dissolved in 95% ethanol, and added to media at a concentration of 10μM and 1μM, respectively. BMP4 and TGFb1 were purchased from R&D, resuspended according to manufacturer's instructions in reconstitution buffer (4mM hydrochloric acid and 0.1% bovine serum albumin), and added to media at a final concentration of 20 ng/ml and 2 ng/ml, respectively.

Skeletal analysis

E18.5 embryos

Alcian blue and alizarin red skeletal staining of E18.5 embryos was performed as described with slight modifications (McLeod, 1980). Briefly, E18.5 embryos were dissected and placed in tap water at 4°C for approximately 4-6 hours before being scalded in 70°C water for approximately 30 seconds. The embryos were then skinned and eviscerated through a hole in the abdomen. Embryos were subsequently fixed in 95% ethanol for 5 days, placed in acetone for 2 days, and stained for 3-4 days in staining solution (1 volume 0.3% alcian blue GS in 70% ethanol, 1 volume 0.1% alizarin red S in 95% ethanol, 1 volume acetic acid, 17 volumes 70% ethanol) at 37°C. Following staining, embryos were washed in distilled water, and cleared in a 1% aqueous solution of KOH for ~36 hours or until the skeleton was visible through the

surrounding tissue. Embryos were then cleared through 20%, 50%, and 80% glycerol:1% aqueous KOH solutions until the surrounding tissue was removed and the skeleton looked clean. Clearing solution was changed every other day. Skeletons were stored and photographed in 100% glycerol.

E15.5 embryos

E15.5 embryos were dissected in PBS and fixed in 95% ethanol for 7 days without skinning or evisceration. Embryos were placed in acetone for 7 days and stained for 3 days as described in the preparation of E18.5 skeletons above. After washing with distilled water, embryos were placed in a 20% glycerol: 2% aqueous KOH solution for 2-3 weeks until the skeleton was visible. Embryos were then cleared through a 50% and 80% glycerol: 1% KOH solution, and stored in 100% glycerol as described above. The gut was removed at the midpoint of this procedure to facilitate clearing.

Establishment of primary mesenchymal cultures

Primary cells were isolated from murine limb buds as previously described (Hoffman et al., 2006). Briefly, whole limbs were removed from E11.5 mouse embryos in ice-cold PBS by squeezing with forceps and torn into small pieces or micro-dissected into proximal and distal regions as indicated in Figure 2 and S1. *Cyp26b1*$^{+/+}$ and *Cyp26b1*$^{+/-}$ limbs were pooled. Limb pieces were proteolytically digested in a dispase solution (10% dispase (Invitrogen, 12mg/ml), 10% FBS, in PSA) with gentle shaking at 37°C. Cells were filtered through a cell strainer (40 µM, Falcon) to obtain a single-cell suspension and were resuspended at a density of $2.0x10^7$ cells/ml. 10µL spots, or "micromasses", were dispensed onto Nunclon delta SI plates – 1 spot/well in a 24-well plate for PNA and alcian blue staining, luciferase assays, and immunofluorescence, and 4-6 spots/well in a 6-well plate for RNA collection. Cells were

incubated at 37°C with 5% CO_2 and allowed to adhere for 1 hour before addition of culture medium (40% DMEM, 60% F12, 10% FBS, Invitrogen) with or without addition of factors. Addition of media was considered time 0 and media was changed every other day following establishment of cultures.

Reporter-based assays

Plasmid constructs

To assess chondrogenic activity, a SOX-responsive reporter was used as described (Weston et al., 2002). This reporter contains 4 re-iterated binding sites for SOX5, 6, and 9 (4x48 base pairs derived from the *Col2a1* gene) upstream of a minimal type II collagen promoter (-89 to +6) coupled to a firefly luciferase gene. A trimerized RARE upstream of firefly luciferase gene (pGL3-RARE-luciferase) was used to assess RA activity (Hoffman et al., 2006).

Transfection of cultures

Primary limb mesenchymal cultures were transiently transfected with Effectene (Qiagen) using a modified protocol as described (Karamboulas et al., 2010). In brief, x µg of DNA (3:1 gene of interest: reporter (9:1 plasmid reporter: pRL-SV40 (Promega))) was incubated with 15x µl of EC buffer (supplemented with 0.4M Trehalose for a higher transfection efficiency, as explained in Garcha and Underhill -in preparation) and x µl enhancer for 10 minutes at room temperature. 5x µl of Effectene was then added, mixed, and incubated for 10 minutes at room temperature, before transferring 15x µl of this mixture to 70x µl of cell suspension. Cells and transfection mix were gently triturated and micromasses plated as described.

Analysis of reporter gene activity

Analysis of reporter gene activity was performed using the Dual Luciferase Reporter Assay System (Promega), according to manufacturer's instructions. Extracts for luciferase were

collected on day 1, 2, 3, or 8, as indicated; cells were washed with PBS, lysed in 100µl of Passive Lysis buffer for 20 minutes, and frozen at -80°C overnight. Firefly and renilla luciferase activity were determined using 20µl of lysate in a 96-well plate reading luminometer (Molecular devices) and firefly luciferase was normalized against Renilla luciferase activity to control for differences in transfection efficiency and to generate relative light units (RLU).

Staining of micromass cultures

Peanut agglutinin (PNA) staining

Primary cultures were washed with PBS and fixed in 4% PFA for 30 minutes at 4°C. Cells were washed with PBS and rhodamine-labeled PNA (Vector Labs, 10µg/ml in PBS) was added to cultures and incubated overnight at 4°C. The following morning, cultures were washed with PBS and the distribution of PNA bound cells was visualized with fluorescence microscopy.

Alcian blue staining

Alcian blue staining of micromass cultures was performed as described in (Weston et al., 2000). Micromasses were washed with PBS and fixed in 95% ethanol at -20°C overnight. Ethanol was removed and cells were washed first with PBS and then with 0.2M HCl for 5 minutes before addition of stain (4 volumes 0.2M HCl, 1 volume alcian blue (0.5% alcian blue 8 GS in 95% ethanol, filtered)). Micromasses were stained overnight, rinsed with 70% ethanol, and stored and photographed in 70% ethanol.

Immunofluorescence

Primary cultures were washed with PBS and fixed in 4% PFA for 30 minutes at 4°C. Cells were washed with PBS, rinsed with distilled water, and antigen retrieval was performed via PK digestion (20µg pK/ml in TE buffer (50mM tris base, 1mM EDTA, 0.5% tritonX-100, pH 8.0) for 10 minutes at 37°C). Cells were then rinsed in PBST, blocked in 1% BSA with 0.3M

glycine, and incubated with an anti-MMP13 antibody (Abcam, ab39012, 1:500, Cambridge, MA) overnight in 1% BSA at 4°C. The following day, cells were rinsed in PBS, incubated with Alexa fluor 488 (Molecular Probes, A11034, 1:1000) in PBS for 1 hour at 4°C, rinsed in PBS, and MMP13 distribution was visualised and photographed using fluorescence microscopy. Control consisted of incubation with the secondary antibody alone.

RNA isolation

RNA isolation from primary cell cultures

RNA was harvested from primary cultures using RNeasy (Qiagen) as per manufacturer's instructions. Cells were washed twice with PBS and the media was aspirated from each well before the addition of 350µL lysis buffer/well of a 6-well plate. After isolation, RNA was resuspended in 30µL of DEPC-treated water and the quality and amount of RNA was assessed using a NanoDrop ND-1000 spectrophotometer.

RNA isolation from tissue

RNA was isolated directly from mouse limbs using Trizol (Invitrogen). The tissue was mixed with 1:10 ratio of tissue volume: Trizol, 20% volume of chloroform added to samples, spun, and the aqueous phase transferred to a new tube. At this point, an equal volume of 70% ethanol was added and the mixture was transferred to the RNAeasy column and procedures followed as described above.

RT-qPCR

Total RNA was isolated as described above and was reverse transcribed to cDNA using the High Capacity cDNA Reverse Transcription kit (Applied Biosystems) as per manufacturer's instructions. Approximately 2µg or the maximum amount of RNA was transcribed in a 20µl reaction volume. To follow the expression of various gene transcripts, quantitative real-time

PCR was carried out using the 7500 Fast Real-Time PCR System (Applied Biosystems). Some primers and TaqMan minor-groove-binding probes were designed using Primer Designer 2.0 (Applied Biosystems) as previously described (Weston et al., 2002; Hoffman et al., 2006; Scott et al., 2010). The primer and probe concentrations were optimized according to the manufacturer's instructions. Other primer and probe sets were designed using IDT RealTime PCR Assay Design Tool or purchased from the TaqMan gene expression collection (Applied Biosystems). Primer and probe sequences that were custom-made are listed in Table 3. Quantification was carried out using ~10 ng of total RNA using the standard curve method and expression of all genes relative to endogenous rRNA was determined using TaqMan Ribosomal Control Reagents (Applied Biosystems).

LacZ staining

E11.5-E14.5 embryos were dissected in PBS and fixed in 0.2% glutaraldehyde in PBS for 30 minutes at room temperature. Fixative was removed, embryos were washed in PBS, and covered in staining solution (2mM MgCl2, 0.02% NP40, 0.01% deoxycholate, 5mM potassium ferrocyanide, 5mM potassium ferricyanide, 0.1% X-gal). Embryos were incubated in staining solution for 4-6 hours at 37°C in a humidified chamber, following which the staining solution was removed, embryos washed in PBS, and fixed overnight in 10% formalin at 4°C. The following day, embryos were washed with PBS, photographed, and stored in 70% ethanol at 4°C.

Microscopy and image acquisition

Images were acquired with a Q-imaging Retiga 1300i camera using Openlab5 Software, through either a dissecting microscope (Stemi SVII, Carl Zeiss Microimaging, Inc.) or an inverted microscope (Axiovert S100, Carl Zeiss MicroImaging, Inc). The *Cyp26b1*$^{-/-}$*/ScxGFP*$^{+}$

fluorescence images were obtained with a Leica MZFLIII (Richmond Hill, ON), using Q-imaging Retiga 2000R and Q-Capture Pro (Q-Imaging, Surrey, BC) software. Images were edited using Adobe Photoshop CS4 (Adobe Systems Incorporated, San Jose, CA) and all images in one panel were adjusted equally.

Statistical analysis

Luciferase assays, immunofluorescence, and alcian blue and PNA staining of micromass cultures were performed in triplicate or quadruplicate and repeated using at least three distinct preparations of cells. RT-qPCR of cultured cells was carried out in duplicate and repeated a minimum of three times with independent RNA samples. RT-qPCR using RNA isolated from tissues was performed on single embryos and repeated with similar results for a minimum of n=3. For studies involving LacZ or skeletal staining of embryos, n=3. One representative experiment is shown for all results.

Data was analysed using a student's t-test with unequal variance or one-way analysis of variance (ANOVA), followed by Tukey post-test for multiple comparisons, using GraphPad Prism, version 5 (GraphPad Software, Inc., La Jolla, CA). Significance is represented as follows: *$p<0.05$, **$p<0.01$, #$p<0.001$.

Table 1. Generation of embryonic genotypes

Embryonic genotype	Father genotype	Mother genotype
Cyp26b1$^{-/-}$	*Cyp26b1* $^{+/-}$	*Cyp26b1* $^{+/-}$
Cyp26b1$^{-/-}$*/ Prrx1Cre*$^{+}$	*Cyp26b1* $^{fl/+}$ */ Prrx1Cre* $^{+}$	*Cyp26b1*$^{fl/fl}$
Cyp26b1$^{-/-}$ */RARE-LacZ*$^{+}$	*Cyp26b1*$^{+/-}$ */ RARELacZ* $^{+}$	*Cyp26b1*$^{+/-}$
Cyp26b1$^{fl/fl}$*/Prrx1Cre*$^{+}$*/RARELacZ*$^{+}$	*Cyp26b1*$^{fl/+}$ */Prrx1Cre*$^{+}$*/RARELacZ*$^{+}$	*Cyp26b1*$^{fl/fl}$
Cyp26b1$^{-/-}$*/ScxGFP*$^{+}$	*Cyp26b1*$^{+/-}$*/ScxGFP*$^{+}$	*Cyp26b1* $^{+/-}$

Table 2. Genotyping parameters

Gene	Primers (5'…3')	Amplicon sizes (bp)	PCR Conditions
Cyp26b1 (MacLean et al., 2007)	Primer 1 CAGTAGATGTTTGAGTGACACAGCC Primer 2 GAGGAAGTGTCAGGAGAAGTGG Primer 3 GGGCCACCAAGGAAGATGCTGAGG	Wildtype 223 Floxed 284 Null 364	94°C 2 min 94°C 20 sec 58°C 50 sec 72°C 45 sec X35 72°C 2 min
Cre Modified from Jax	Forward GCGGTCTGGCAGTAAAAACTATC Reverse GTGAAACAGCATTGCTGTCACTT	Cre^+ 100	94°C 3 min 94°C 20 sec 51°C 1 min 72°C 40 sec X35 72°C 3 min
LacZ Modified from Jax	Forward ATCCTCTGCATGGTCAGGTC Reverse CGTGGCCTGATTCATTCC	$LacZ^+$ 315	94°C 3 min 94°C 20 sec 58°C 30 sec 72°C 35 sec X 25 72°C 2 min
GFP Modified from Jax	Forward AAGTTCATCTGCACCACCG Reverse TCCTTGAAGAAGATGGTGCG	GFP^+ 173	94°C 3 min 94°C 30 sec 60°C 1 min 72°C 1 min X 35 72°C 2 min

Table 3. Primers and probes designed for RT-qPCR

Gene	Forward primer (5'-3')	Reverse primer (5'-3')	Probe (5'-3')	System
Acan	AGGTTGCTATGGTGACAAGG	TGGAAGGTGAATTTCTCTGGG	6FAM/TCGCTGAGG/ZEN/AGATGGAGGGTGA/IABkFQ	IDT
Col1a1	CTTCACCTACAGCACCCTTGTG	TTGGTGGTTTTGTATTCGATGACT	6FAM/ACACCGGAACTTGGG/MGBNFQ	ABI
Col2a1	GGCTCCCAACACCGCTAAC	GATGTTCTGGGAGCCCTCAGT	6FAM/CAGATGACTTTCCTCCGTC/MGBNFQ	ABI
Comp	CCAGAAAGATAACCCAGACCAG	GTGACCATCCCCATCCTG	6FAM/ACAGGCATC/ZEN/ACCCACAAAGTCGT/IABkFQ	IDT
Cspg4	CCTTCACGATCACCATCCTTC	AATCATTGTCTGTTCCCCTGAG	6FAM/ATGACCAAC/ZEN/CCCCTGTTCTCACC/IABkFQ	IDT
Cyp26a1	CTCCAACCTGCACGATTCCT	CGGCTGAAGGCCTGCAT	6FAM/CAGCGAAAGAAGGTG/MGBNFQ	ABI
Cyp26b1	CCTGAGGCCATCAATGTATATCAG	CACACGCACGGCCATTC	6FAM/CCCAGCGACTTACCT/MGBNFQ	ABI
Hapln1	GTGAGGTGATTGAAGGGCTAG	CAGTCGTGGAAAGTAAGGGAA	6FAM/TGGCATTGG/ZEN/AGTTACAAGGTGTGGT/IABkFQ	IDT
Ihh	CCCAACTACAATCCCGACATC	TCACCCGCAGTTTCACAC	6FAM/CCGACCGCC/ZEN/TCATGACCCA/IABkFQ	IDT
Matn1	GATAGCCTCAGTCTTGTCCC	CCTTCACCTTCTCAAACTCCAC	6FAM/AAACACCAG/ZEN/GTCCGTGGGTCG/IABkFQ	IDT
Mkx	ACGTTCAGTGGTTTCCTGG	CTTATGCCTTACCTTCCCTCC	6FAM/CGCCCCTCA/ZEN/AGGACAACCTCA/IABkFQ	IDT
Ptch1	CTGCCTGTCCTCTTATCCTTC	AGACCCATTGTTCGTGTGAC	6FAM/CTGCCCACT/ZEN/CCTTCGCCTGA/IABkFQ	IDT
Pth1r	ATGCTCTTCAACTCCTTCCAG	ACTCCCACTTCGTGCTTTAC	6FAM/CGGCTCCAA/ZEN/GACTTCCTAATCTCTGC/IABkFQ	IDT
Rarb	ATTAAGATCGTGGAGTTCGCC	AGTCATGGTGTCTTGCTCTG	6FAM/AGGGTGATC/ZEN/TGGTCTGCGATGG/IABkFQ	IDT
Runx2	TCCCCGGGAACCAAGAA	GCGATCAGAGAACAAACTAGGTTTAGA	6FAM/CACAGACAGAAGCTTGATGA/MGBNFQ	ABI
Sox5	TGCTTACTGACCCTGATTTACC	TCTCCATCTGTCTCCCCATAC	6FAM/ATGTCTTCC/ZEN/AAGCGACCAGCCT/IABkFQ	IDT
Sox9	CATCACCCGCTCGCAATAC	CCGGCTGCGTGACTGTAGTA	6FAM/ACCATCAGAACTCCGGCT/MGBNFQ	ABI

Gene	Forward primer (5’-3’)	Reverse primer (5’-3’)	Probe (5’-3’)	System
Spp1	GTGATTTGCTTTTGCCTGTTTG	GAGATTCTGCTTCTGAGATGGG	6FAM/CCCTCCCGG/ZEN/TGAAAGTGACTGATT/IABkFQ	IDT
Tnc	ATAGCCAACATCACAGACTCAG	GCTCGTACTCCACTGTATTTCC	6FAM/TGTAACTTC/ZEN/TGGCACTCTCTCCCCT/IABkFQ	IDT
Vcan	ACCTCACAAGCATCCTTTCTC	GGGTCTCCAGTTCTCATATTGC	6FAM/TCATGGCCC/ZEN/ACACGATTCACAAAC/IABkFQ	IDT

CHAPTER 3: RESULTS

Prrx1Cre^{+}*/Cyp26b1*$^{-/-}$ mice exhibit limb malformations less severe than *Cyp26b1*$^{-/-}$ mice

Cyp26b1 is the primary RA-metabolizing enzyme in the developing limb bud. To further examine the role of endogenous retinoid signalling in skeletogenesis, both conventional and conditional *Cyp26b1* knockout mice were analyzed. *Cyp26b1*$^{fl/fl}$ mice were crossed with *PcxNLSCre*$^{+}$ transgenic mice in order to achieve deletion of *Cyp26b1* in the germline and to generate *Cyp26b1* null animals. These animals exhibited marked developmental malformations as previously described (Yashiro et al., 2004; Pennimpede et al., 2010b). *Cyp26b1*$^{fl/fl}$ mice were also crossed with a line of transgenic mice that express Cre under direction of the *Prrx1* promoter, which is expressed as early as E9.5 in the developing limb bud, parts of the head, and sternum (Logan et al., 2002; Kimura et al., 2010). By external observation, both *Cyp26b1*$^{-/-}$ and *Prrx1Cre*$^{+}$*/Cyp26b1*$^{fl/fl}$ mice exhibited truncated limbs and abnormal digit formation at E18.5, although the limbs of *Prrx1Cre*$^{+}$*/Cyp26b1*$^{fl/fl}$ mice were not as severely truncated and presented with more digits than age-matched *Cyp26b1*$^{-/-}$ animals (Figure 4A). Wildtype littermates in *Prrx1Cre*$^{+}$*/Cyp26b1*$^{fl/fl}$ and *Cyp26b1*$^{-/-}$ lines were both morphologically normal and comparable for experimental purposes (Appendix 1A).

At E18.5, *Cyp26b1*$^{-/-}$ mice exhibit a greatly reduced stylopod and zeugopod, a loss of carpal bones, and oligodactyly, with only 2 or 3 digits forming per autopod. *Prrx1Cre*$^{+}$*/Cyp26b1*$^{fl/fl}$ animals present with a slightly longer stylopod and zeugopod than null animals, recognizable wrist elements, and the formation of 4 digits (Figure 4B). In both lines, the scapula and ilium appear morphologically normal, and nail-like structures are formed at the digit tips (data not shown). The clavicle is missing in *Cyp26b1*$^{-/-}$ but this structure is not deleted in *Prrx1Cre*$^{+}$*/Cyp26b1*$^{fl/fl}$ animals.

While the fore- and hindlimb have a similar phenotype in null animals, the hindlimb appears to be more severely affected in *Prrx1Cre*$^{+}$*/Cyp26b1*$^{fl/fl}$ animals, as the radius and ulna can be identified in the forelimb zeugopod, but the fibula/tibia are not distinguishable in the hindlimb zeugopod. In addition, both the stylopod and zeugopod in the forelimb are not as severely truncated as in null animals, but this is only true for the stylopod in *Prrx1Cre*$^{+}$*/Cyp26b1*$^{fl/fl}$ animals. Furthermore, while both fore- and hindlimbs have the formation of 4 digits, those that form in the forelimb appear morphologically normal, whereas the hindlimb digits are partially fused together.

The defects described at E18.5 are apparent as early as E15.5, and notably, areas of alizarin red staining in wild-type skeletons are not present in either the *Prrx1Cre*$^{+}$*/Cyp26b1*$^{fl/fl}$ or *Cyp26b1*$^{-/-}$ animals at E15.5 (Figure 4C). These areas of staining are observable at E18.5, indicating a delay in the mineralization of skeletal elements in both Cyp26b1 conditional and null mutants. Furthermore, *Prrx1*-Cre driven deletion of *Cyp26b1* partially rescues both the autopod and to a lesser extent the stylopod defects, whereas the zeugopod is substantially impacted in both transgenic lines.

Levels of retinoid signaling are increased in *Cyp26b1*$^{-/-}$ limb buds and to a lesser extent in *Prrx1Cre*$^{+}$*/Cyp26b1*$^{fl/fl}$ animals

The limbs of the *Prrx1Cre*$^{+}$*/Cyp26b1*$^{fl/fl}$ mice were less severely affected than *Cyp26b1*$^{-/-}$ limbs, and to determine if differences in RA signalling contributed to these phenotypes, both lines were crossed with an RA reporter transgenic mouse. Limbs from *Prrx1Cre*$^{+}$*/Cyp26b1*$^{fl/fl}$ and *Cyp26b1*$^{-/-}$ animals expressing the RARE-LacZ transgene, which harbours a trimerized repeat of RARb2 RARE linked to the *hsp68* minimal promoter (Rossant 1991), were stained for X-gal to allow visualization of activated retinoid signalling. Fore- and

hindlimbs exhibited similar patterns of retinoid signalling. At E11.5, very little staining is observed in the limbs of wild-type mice, but is present proximally in *Cyp26b1*$^{-/-}$ limbs (Appendix 1B). By E12.5, activated RA signaling can be observed in the interdigital region of wild-type limbs; however, in null animals, areas showing activated retinoid signalling extend almost throughout the entire proximal-distal axis of the limb bud (Figure 5A). In *Prrx1Cre*$^{+}$*/Cyp26b1*$^{fl/fl}$ animals, aberrant retinoid signalling is observed proximally, but this is not as intense, and does not expand as far distally, as in the null animals. At E13.5 and E14.5, retinoid signalling continues to be observed interdigitally in wildtype limbs, while the only area free of activated retinoid signalling in *Cyp26b1*$^{-/-}$ limbs is the very distal tip, where *Cyp26a1* is expressed (Abu-Abed et al., 2002) (Figure 5A and Appendix 1B). Again, *Prrx1Cre*$^{+}$*/Cyp26b1*$^{fl/fl}$ limbs exhibit "intermediate" levels (in terms of both distribution pattern and intensity) of activated retinoid signaling between wild-type and *Cyp26b1*$^{-/-}$ limbs.

In order to further investigate changes in RA signalling in the mutant limbs, fore- and hindlimb buds were microdissected into proximal and distal regions for analysis of *Cyp26b1* and *Rarb* expression. Quantitative RT-PCR (qPCR) demonstrated that *Cyp26b1* is more highly expressed in the distal region of the developing limb bud at E11.5 and E12.5, as previously reported (Yashiro et al., 2004; Pennimpede et al., 2010b), and revealed that while *Cyp26b1* expression is completely absent in *Cyp26b1*$^{-/-}$ animals, *Prrx1Cre*$^{+}$*/Cyp26b1*$^{fl/fl}$ animals have a small amount of *Cyp26b1* expression remaining in the distal regions of the limb (Figure 5B and Appendix 1C). *Cyp26b1* is absent in the proximal regions of *Prrx1Cre*$^{+}$*/Cyp26b1*$^{fl/fl}$ limbs. *Rarb* expression in the proximal and distal regions of fore- and hindlimbs was analysed to determine quantitative increases in retinoid signalling in these tissue populations, as *Rarb* is a direct RAR target gene and is expressed in proximal limb mesenchyme and later in interdigital regions

(Mollard et al., 2000). Large increases in *Rarb* expression were observed in both proximal and distal regions of *Prrx1Cre*$^{+}$*/Cyp26b1*$^{fl/fl}$ and *Cyp26b1*$^{-/-}$ fore- and hindlimbs, although increases in the *Prrx1Cre*$^{+}$*/Cyp26b1*$^{fl/fl}$ limb were not as large, particularly in the distal regions where small amounts of *Cyp26b1* expression was observed.

To further assess retinoid status in the limb mesenchyme, PLM cultures were established from E11.5 wild-type and *Cyp26b1*$^{-/-}$ limbs (Ahrens et al., 1977). These cultures allow for the effects on mesenchyme versus ectoderm to be separated. qPCR analysis revealed that in the absence of *Cyp26b1*, *Cyp26a1* and *Crabp2* expression increased, and *Aldh1a2* expression decreased, likely to compensate for increased levels of RA (Figure 5C and Appendix 1D). Additionally, the expression of direct RAR-target genes *Rarb* and *Fgf18* increased ~ 3-fold at 3 days, indicating increased retinoid signalling occurs in culture (Figure 5C and Appendix 1D). Furthermore, the activity of a retinoid-responsive reporter, RARE-LUC, which consists of a trimerized RARE upstream of the firefly luciferase gene, increased significantly in *Cyp26b1*$^{-/-}$ PLM cultures. Treatment with an ALDH1 inhibitor, diethylaminobenzaldehyde (DEAB) at culture initiation was able to reduce RARE-LUC reporter activity in *Cyp26b1*$^{-/-}$ cultures, but not to wild-type levels (Figure 5D). Altogether, these results indicate increased and sustained endogenous retinoid signalling in *Cyp26b1*$^{-/-}$ limb mesenchyme.

Increased retinoid signalling negatively affects chondrogenesis

It has previously been reported that increased levels of RA negatively affect skeletal development by inhibiting chondrogenesis (Cash et al., 1997; Weston et al., 2000; Weston et al., 2002); however, the role of RA signalling in cartilage formation has not been fully investigated using *in vivo* models. qPCR analysis of microdissected E11.5 and E12.5 limbs from wildtype and *Cyp26b1*$^{-/-}$ embryos demonstrated little change in the expression of chondrogenic marker

Sox9, but *Acan* expression was significantly decreased (Figure 6A). A Col2-LUC reporter, which is based on the SOX5, SOX6, and SOX 9 binding site from the first intron of *Col2a1* upstream of the firefly luciferase gene (Lefebvre et al., 1997; Lefebvre et al., 1998) was used to follow chondoblast differentiation. This reporter has been shown to tightly correlate with chondroblast differentiation and cartilage formation (Weston et al., 2000; Hoffman et al., 2006; Muramatsu et al., 2007). Col2-LUC reporter activity was 7.4-fold less in *Cyp26b1*$^{-/-}$ cultures when compared to wild-type after only 1 day of culture (Figure 6B). Treatment with DEAB was able to increase Col2-LUC activity in both wild-type and null cultures, however, even "rescued" *Cyp26b1*$^{-/-}$ cultures had significantly lower Col2-LUC reporter activity than untreated wild-type cultures (Figure 6B). Notably, Col2-LUC reporter activity is tightly correlated with RA reporter activity, as overexpression of *Cyp26a1*, which degrades RA, leads to a 2-fold decrease in RA reporter activity and a 2-fold increase in Col2-LUC (Figure 6C).

BMPs have been shown to play an essential role in limb skeletogenesis, both in specifying limb mesenchymal cells to a chondrocytic fate and in enhancing their subsequent differentiation into chondroblasts (Yoon and Lyons, 2004; Pogue and Lyons, 2006; Wu et al., 2007). To determine if the "chondrogenic" defect of the *Cyp26b1*$^{-/-}$ mesenchyme could be rescued by BMP addition, null and wild-type PLM cultures were established and treated with or without BMP4. As reported previously, BMP4 reduced the activity of a retinoid responsive reporter gene in wild-type cells and this was also observed albeit to a lesser extent in the *Cyp26b1* null mesenchyme (Figure 6D) (Hoffman et al., 2006). Interestingly, BMP4 exhibited negligible pro-chondrogenic activity in cultures derived from *Cyp26b1* null embryos, whereas BMP4 promoted chondrogenesis in wild-type cultures—determined by following Col2-LUC

reporter activity and alcian blue staining (Figure 6D). These results further demonstrate that the *Cyp26b1* null mesenchyme exhibits a defect in chondrogenesis.

Cyp26b1$^{-/-}$ cells do not progress normally through the chondrogenic program

Previous work has shown a requirement for RAR-mediated repression in chondroblast differentiation *in vitro* (Weston et al., 2000; Weston et al., 2002) and that RA promotes chondrocyte hypertrophy (Koyama et al., 1999). Herein *Cyp26b1* deficient mice have been used as a model to systematically examine the role of endogenous RA signalling in chondrogenesis *in vitro* and *in vivo*.

Cyp26b1$^{-/-}$ *cells are maintained at a pre-chondrogenic stage*

The first step in chondrogenesis is the aggregation of pre-chondrogenic cells into precartilaginous condensations. To normalize for potential differences in cell density which would impact chondrogenesis, *Cyp26b1*$^{+}$ and *Cyp26b1*$^{-/-}$ cultures were plated at similar densities and under these conditions no overt increase in cell death was observed. Following culture of limb mesenchymal cells, peanut agglutinin (PNA) staining was used to identify pre-chondrogenic condensations. These analyses revealed very little difference between the ability of wild-type and *Cyp26b1*$^{-/-}$ cultures to form prechondrogenic condensations following 1 day of culture (Figure 7A). With increased culture time, cells within the condensations typically exhibit reduced PNA staining as they differentiate and this is not observed in the *Cyp26b1*$^{-/-}$ derived cultures, in which PNA staining intensity is maintained. The addition of DEAB had little impact on the condensation of both wild-type and *Cyp26b1*$^{-/-}$ cells (Figure 7A). qPCR analysis revealed that while there is little change in *Sox9* expression between wild-type and *Cyp26b1*$^{-/-}$ cultures, the expression of condensation markers *Vcan* and *Tnc* is maintained or increased in null cultures

(Figure 7B). These results indicate that *Cyp26b1*$^{-/-}$ cells form discrete prechondrogenic condensations that do not progress beyond this stage.

***Cyp26b1*$^{-/-}$ cells exhibit reduced chondroblast differentiation**

To further address the impact of *Cyp26b1* loss on chondrogenesis and specifically chondroblast differentiation and the associated production of a cartilaginous extracellular matrix, PLM cultures were stained with alcian blue. Consistent with the Col2-LUC reporter gene findings in *Cyp26b1*$^{-/-}$ cells (Figure 8A), a marked decrease in alcian blue staining of cartilage nodules is observed in *Cyp26b1*$^{-/-}$ cultures. This is obvious as early as day 4 of culture, and is much more pronounced by day 8. Addition of DEAB results in a small increase in cartilage formation in *Cyp26b1*$^{-/-}$ cultures (Figure 8A). qPCR analysis of *Cyp26b1*$^{-/-}$ cultures demonstrates that *L-Sox5* and *Sox6* expression is reduced ~ 60%. Similarly, the expression of extracellular matrix molecules such as *Col2a1*, *Acan*, *Hapln1*, *Comp*, *Matn1*, and to a lesser extent, *Cspg4* and *Mia1*, were significantly decreased (Figure 8B). These findings are congruent with the analysis of *Sox9* and *Acan in vivo* (Fig. 6A) and are also consistent with the severe defects in the cartilaginous elements in the *Cyp26b1*$^{-/-}$ limbs. Altogether, these results indicate that markers associated with chondroblast differentiation are appreciably decreased in the limb mesenchyme of *Cyp26b1*$^{-/-}$ mice.

***Deletion of Cyp26b1*$^{-/-}$ has a modest impact on chondrocyte hypertrophy**

In contrast to the negative role of RAR activation in chondroblast differentiation, RA signalling has been shown to be important in chondrocyte hypertrophy. There was little change in expression of the hypertrophic markers *Pthr1*, *Vegfa*, and *Runx2* in *Cyp26b1*$^{-/-}$ cells compared to wild-type, however, an increase in *Spp1* and a decrease in *Col10a1*, *Mmp13* and *Alp1* were observed after 8 days of culture (Figure 9A). Notably, the expression of *Ihh* was substantially

down-regulated at all time points in *Cyp26b1*$^{-/-}$ cultures. Consistent with this, the hedgehog target gene *Ptch1* was also decreased. Furthermore, IHH impacts *Pthrp* expression, and *Pthrp* was also found to be significantly down-regulated. *Cyp26b1* null mesenchyme-derived cultures produce fewer cartilage nodules, and as such it might be expected that chondrogenic stages subsequent to chondroblast differentiation such as chondrocyte hypertrophy would be negatively impacted. To determine if the nodules that did form underwent chondrocyte hypertrophy, immunofluorescence was performed to examine the distribution of MMP13 expression. This analysis revealed that there is little change in protein distribution of MMP13 (Figure 9B). These findings suggest that the decrease in many of the hypertrophy-associated genes such as *Mmp13* likely reflects a decrease in number of cartilage nodules, rather than a decrease in hypertrophy.

The impact of manipulation of endogenous retinoid signalling on chondrogenesis and chondrocyte hypertrophy was further explored in PLM cultures treated with ketoconazole, a CYP inhibitor. Analysis of gene expression in wild-type cells treated with ketoconazole demonstrates similar changes in gene expression as observed with *Cyp26b1*$^{-/-}$ cultures (Appendix 2). As ketoconazole inhibits both CYP26A1 and CYP26B1 activity, this highlights the role of *Cyp26a1* expression in the *Cyp26b1*$^{-/-}$ limb. Changes in expression of components of the retinoid signalling indicate increased retinoid signalling, and analysis of genes involved in the chondrogenic program reflect little change in condensation and decreased chondroblast differentiation. More importantly, as observed in the *Cyp26b1*$^{-/-}$ cultures, treatment with ketoconazole leads to a substantial decrease in *Ihh* expression, whereas hypertrophic markers are modestly increased.

The chondrogenic potential of proximal limb cells is more affected by changes in RA signalling

To investigate the effect of modulation of RA signalling on the chondrogenic potential of cells from different regions of the limb, PLM cultures were established from the proximal or distal region of E11.5 wild-type limbs and treated with ketoconazole, a CYP450 inhibitor, or DEAB. This allows for a comparison between the timing of CYP inhibition in the two limb regions. Treatment with ketoconazole results in a decrease in Col2-LUC reporter activity and a correlated increase in RARE-LUC reporter activity. Conversely, treatment with DEAB has the opposite effect. Concentrations of ketoconazole and DEAB were chosen such that treatment would have a pronounced effect on reporter activity and cartilage formation (Appendix 3A). Treatment on day 0 or day 1 had a similar effect on cartilage formation as assessed by alcian blue staining and reporter activity (Appendix 3B and 3C).

Alcian blue staining of differentiated cartilage nodules demonstrated that treatment with ketoconazole results in decreased cartilage formation in both proximal and distal cultures. However, this decrease is observed to a greater extent in the proximally-derived cultures, which are at a different stage within the chondrogenic program. Conversely, treatment with DEAB increases cartilage formation, and also has a more pronounced effect in proximal cultures (Figure 10a). This correlates with the activity of Col2-LUC and RARE-LUC reporters, in which a decrease in Col2-LUC reporter activity and increase in RARE-LUC reporter activity was observed with ketoconazole treatment, and the opposite with DEAB treatment (Figure 10B). Treatment with ketoconazole had a much greater effect in proximally-derived cultures, with a 6.3 versus 2.0-fold change in Col2-LUC reporter activity and a 5.0 versus 2.7-fold change in RARE-LUC reporter activity in proximal and distal cultures, respectively. Treatment with DEAB had similar effects on RARE-LUC activity in proximal and distal cultures, however, proximal

cultures exhibited a greater difference in Col2-LUC reporter activity versus distal cultures (2.6 versus 1.2-fold change). qPCR analysis demonstrates that *Cyp26b1* increased with ketoconazole treatment and decreased with DEAB treatment, consistent with previous reports (Hoffman et al., 2006) (Figure 10C). This occurs in both proximal and distal regions of the limb, with greater changes observed in proximally-derived cultures. Analysis of chondrogenic marker expression in proximally-derived cultures mimics that seen in *Cyp26b1*$^{-/-}$ cultures, with little change in *Sox9* expression, but a decrease in markers associated with chondroblast differentiation.

Increased expression of tendon markers in *Cyp26b1*$^{-/-}$ animals

The decrease in chondrogenic markers in *Cyp26b1*$^{-/-}$ cultures and the relatively small decreases in *Sox* genes led to the hypothesis that mesenchymal cells in *Cyp26b1*$^{-/-}$ animals are being maintained as chondroprogenitors, multi-potent progenitors or are being specified to an alternate cell fate. To address this possibility we examined the expression of other mesenchymal lineage markers, such as those associated with tendogenesis, as the *Sox* factors are expressed in this lineage (Soeda et al., 2010). Analysis of tendon markers in *Cyp26b1*$^{-/-}$ PLM culture by qPCR revealed an increase in *Scx*, *Tnmd*, and *Col1a1* expression, and other markers of tendon development, in null cultures (Figure 11A and Appendix 4A) (Xu et al., 1997; Schweitzer et al., 2001; Docheva et al., 2005)). Visualisation of *Scx* expression, which is expressed in tendon progenitors, in *Cyp26b1*$^{-/-}$ animals expressing the *ScxGFP*$^{+}$ transgene (Schweitzer et al., 2001; Pryce et al., 2007) demonstrates that *Scx* expression is increased in the forelimb of null animals when compared to wild-type littermates (Figures 11B and 11C). qPCR analysis of *Scx* expression in fore- and hindlimbs microdissected into proximal and distal regions also demonstrates that *Scx* expression is modestly increased in *Cyp26b1*$^{-/-}$ animals (Figure 11D).

To further examine the effect of retinoid signalling on tendon marker expression, PLM cultures established from the limbs of *ScxGFP*$^{+}$ mice were treated with ketoconazole or DEAB in order to assess the distribution of *Scx* expression following modulation of endogenous RA signalling. *Scx* is excluded from developing cartilage nodules as reported previously (Asou et al., 2002) and a notable increase in EGFP expression is apparent in ketoconazole treated cultures. Conversely, treatment with DEAB leads to a reduction in EGFP expression (Figure 10E). Consistent with these findings, qPCR analysis of wild-type PLM cultures treated with ketoconazole demonstrate a significant increase in *Scx* expression after 1 and 3 days of culture; however, this is only apparent in cultures derived from the proximal region of the limb (Figure 10F). Conversely, treatment with DEAB leads to a reduction in *Scx*, *Col1a1*, and *Tnmd* expression in proximal cultures after 3 days (Figure 10F and Appendix 4B).

TGFβ is a potent inducer of *Scx* expression, while BMPs negatively regulate the induction of tendon primordium in the limb (Schweitzer et al., 2001; Pryce et al., 2007). Treatment of PLM cultures established from *ScxGFP*$^{+}$ embryos with TGFβ1 or BMP4 resulted in an increase and decrease, respectively, in EGFP expression. Notably, treatment with both TGFβ1 and BMP4 results in little EGFP expression, while treatment with both ketoconazole increased the ability of TGFβ1 to induce *Scx* expression (Figure 10G). Alcian blue staining demonstrates that cultures treated with compounds promoting *Scx* expression result in less cartilage formation, and vice versa (Appendix 4C). Together, these results indicate that increased retinoid signalling in the limb mesenchyme positively influences tendogenesis.

Figure 4. Limb malformations are less severe in *Prrx1Cre*$^{+/}$*Cyp26b1*$^{fl/fl}$ mice than *Cyp26b1*$^{-/-}$ mice.

A) External appearance of E18.5 embryos. B) Alcian blue and alizarin red staining of E18.5 skeletons. C) Alcian blue and alizarin red staining of E15.5 skeletons. The left limb is shown in all cases. Scale bar, 3.5mm. FL, forelimb; HL, hindlimb.

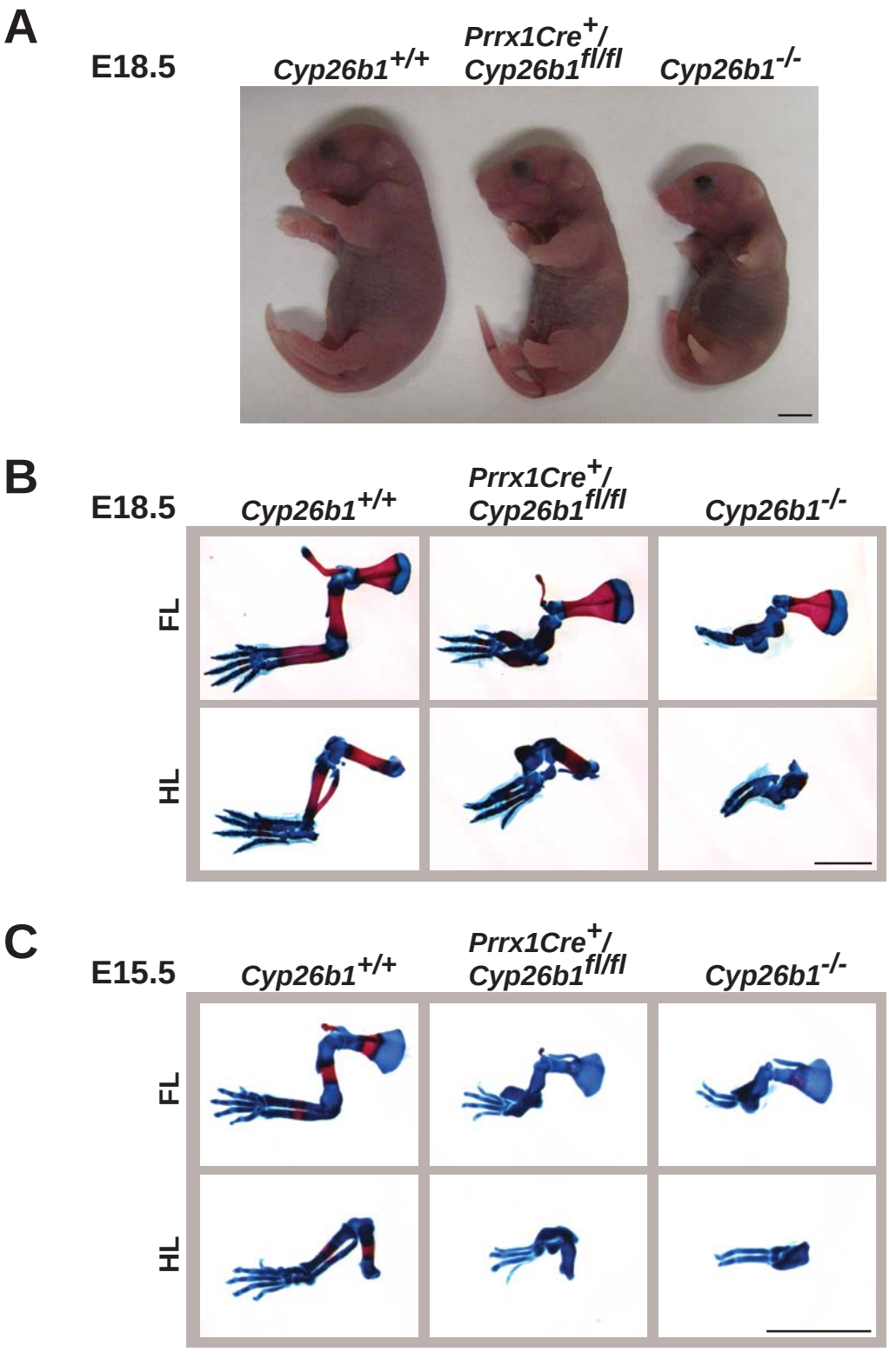
A
E18.5
Cyp26b1+/+
Prrx1Cre+/
Cyp26b1fl/fl
Cyp26b1-/-
B
E18.5
Cyp26b1+/+
Prrx1Cre+/
Cyp26b1fl/fl
Cyp26b1-/-
FL
HL
C
E15.5
Cyp26b1+/+
Prrx1Cre+/
Cyp26b1fl/fl
Cyp26b1-/-
FL
HL

Figure 5. Retinoid signalling is increased in *Cyp26b1*$^{-/-}$ limbs and to a lesser extent in *Prrx1Cre*$^{+/}$*Cyp26b1*$^{fl/fl}$ limbs.

A) X-gal staining of E12.5 and E14.5 limbs from wildtype, *Prrx1Cre*$^{+}$*/Cyp26b1*$^{fl/fl}$, and *Cyp26b1*$^{-/-}$ mice heterozygous for the RARE-LacZ transgene. A dorsal view of the left limb is shown. B) Schematic representation an E12.5 limb bud showing the cuts made to generate forelimb proximal (FP) and distal (FD) and hindlimb proximal (HP) and distal (HD) regions. Analysis of *Cyp26b1* and *Rarb* expression in these four regions of E12.5 limb buds by qPCR. Analysis was performed on single embryos and repeated with similar results. C) qPCR analysis of *Cyp26a1*, *Aldh1a2*, and *Rarb* expression in PLM cultures after 1 or 3 days of culture. D) RARE-LUC reporter activity in PLM cultures after 1, 3, or 8 days of culture, in the presence or absence of DEAB (10μM). Control was set as 100% for *Cyp26b1*$^{+}$ on day 1. Scale bar, 2mm. Error bars represent 1 s.d. Significance was evaluated in comparison to wildtype untreated controls on the same day and is represented as follows: *$p<0.05$; **$p<0.01$; $^{\#}p<0.001$. FL, forelimb; HL, hindlimb; P, proximal; D, distal. Nd, 40 cycles of qPCR and transcript not detected; Rel. Express., relative expression; RLU, relative light units.

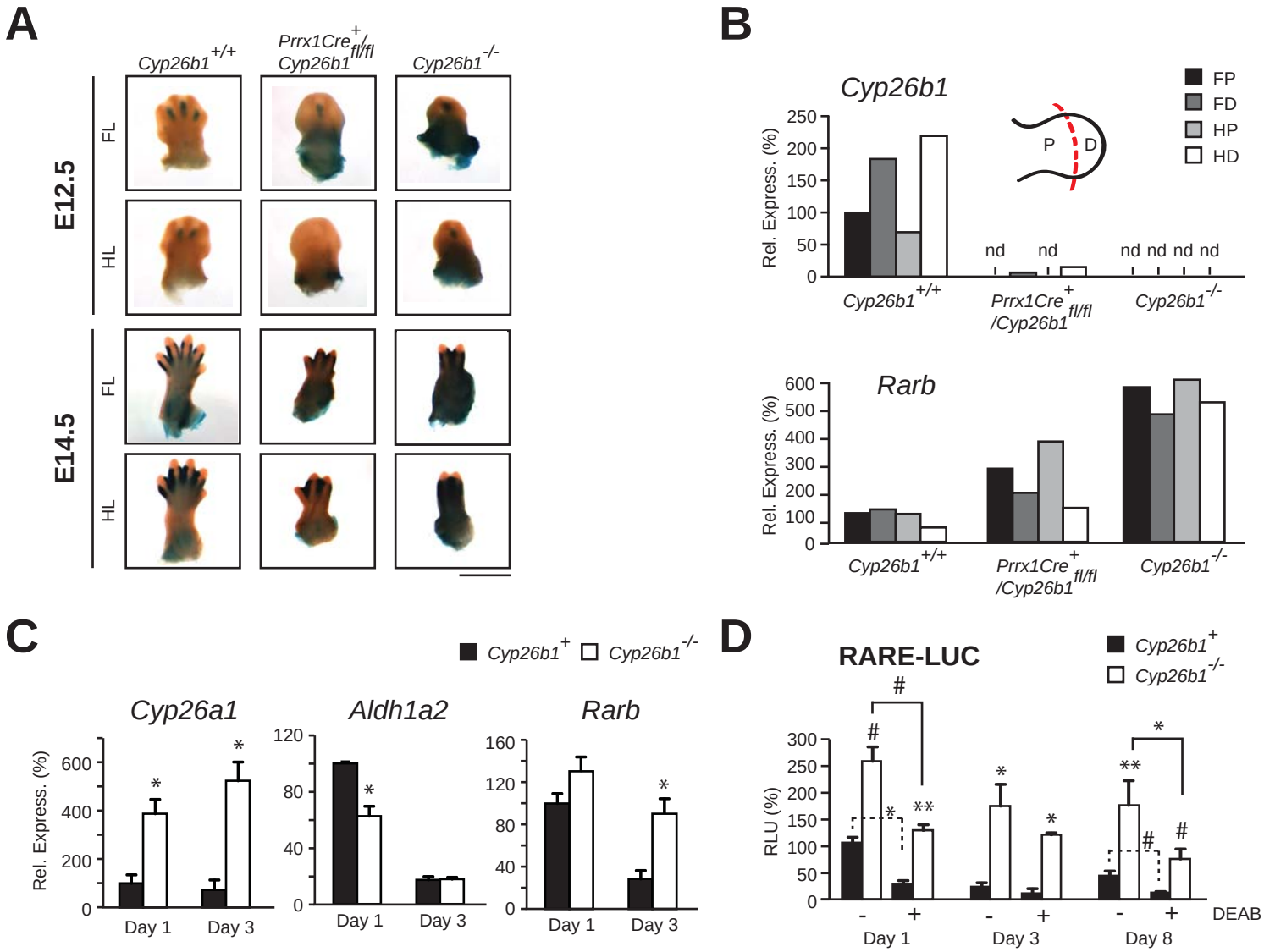
A
Cyp26b1+/+
Prrx1Cre+/ Cyp26b1fl/fl
Cyp26b1-/-
E12.5
E14.5
FL
HL
B
Cyp26b1
FP
FD
HP
HD
Rel. Express. (%)
P
D
nd
Cyp26b1+/+
Prrx1Cre+/Cyp26b1fl/fl
Cyp26b1-/-
Rarb
C
Cyp26b1+
Cyp26b1-/-
Cyp26a1
Aldh1a2
Rarb
Day 1
Day 3
D
RARE-LUC
RLU (%)
DEAB
Day 8

Figure 6. Chondrogenesis decreases in response to elevated levels of RA signalling.

A) qPCR analysis of *Sox9* and *Acan* expression in FP, FD, HP, and HD regions of E11.5 and E12.5 limb buds. B) A *Col2a1*-derived reporter gene (Col2-LUC) was used to follow SOX5, 6, and 9 activity in PLM cultures after 1, 3, or 8 days of culture with or without DEAB treatment (10µM). Control was set as 100% for *Cyp26b1*$^{+}$ on day 1. C) Col2-LUC and RARE-LUC reporter activity after two days of culture following transient transfection of *Cyp26a1* in PLM cultures. D) Col2-LUC and RARE-LUC reporter activity following treatment with BMP4 (B4, 20 ng/ml). Luciferase extracts were collected on day 3. Alcian blue staining of 4 day-old PLM cultures treated with BMP4. Error bars represent 1 s.d. Significance was evaluated in comparison to wildtype untreated controls on the same day and is represented as follows: *$p<0.05$; **$p<0.01$; $^{\#}p<0.001$.

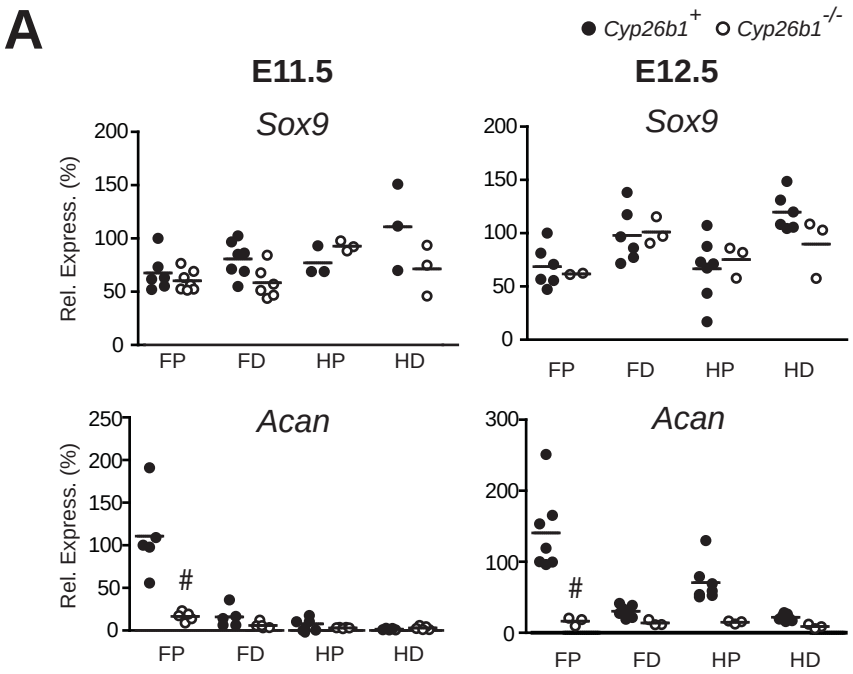
A
Cyp26b1+ Cyp26b1-/-
E11.5
E12.5
Sox9
Acan
Rel. Express. (%)
FP
FD
HP
HD

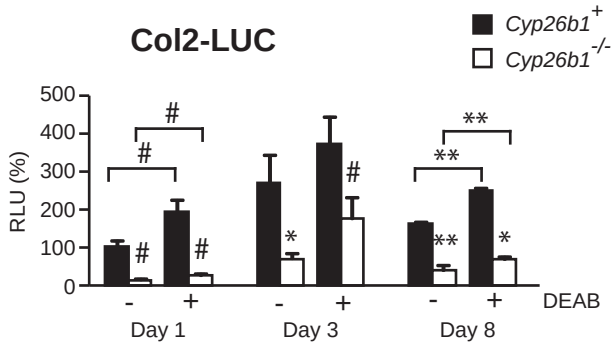
B
Col2-LUC
Cyp26b1+
Cyp26b1-/-
RLU (%)
Day 1
Day 3
Day 8
DEAB

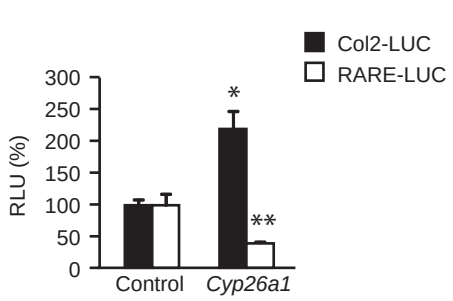
C
Col2-LUC
RARE-LUC
RLU (%)
Control
Cyp26a1

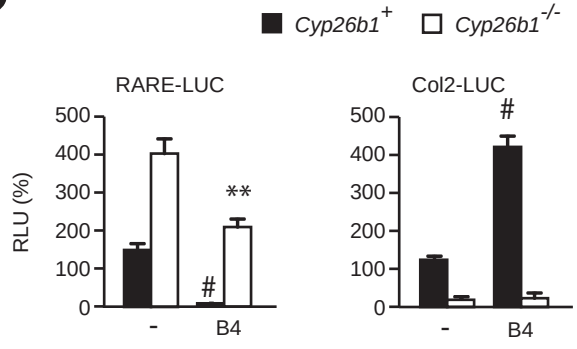
D
Cyp26b1+
Cyp26b1-/-
RARE-LUC
Col2-LUC
RLU (%)
B4

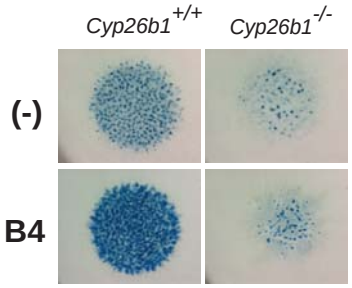
Cyp26b1+/+
Cyp26b1-/-
(-)
B4

Figure 7. Cells from *Cyp26b1*$^{-/-}$ limb mesenchyme express/retain markers indicative of pre-cartilaginous condensations

A) Peanut agglutinin (PNA) staining of PLM cultures treated with or without DEAB (10μM) for 1 or 5 days. Day 1 cultures were photographed with a higher exposure than day 5 cultures. B) qPCR analysis of condensation markers *Sox9*, *Vcan*, *Tnc*, and *Twist1* in PLM cultures after 1 or 3 days of culture. Scale bar, 200μm. Error bars represent 1 s.d. Significance was evaluated in comparison to wildtype controls on the same day and is represented as follows: *$p<0.05$; **$p<0.01$; $^{\#}p<0.001$.

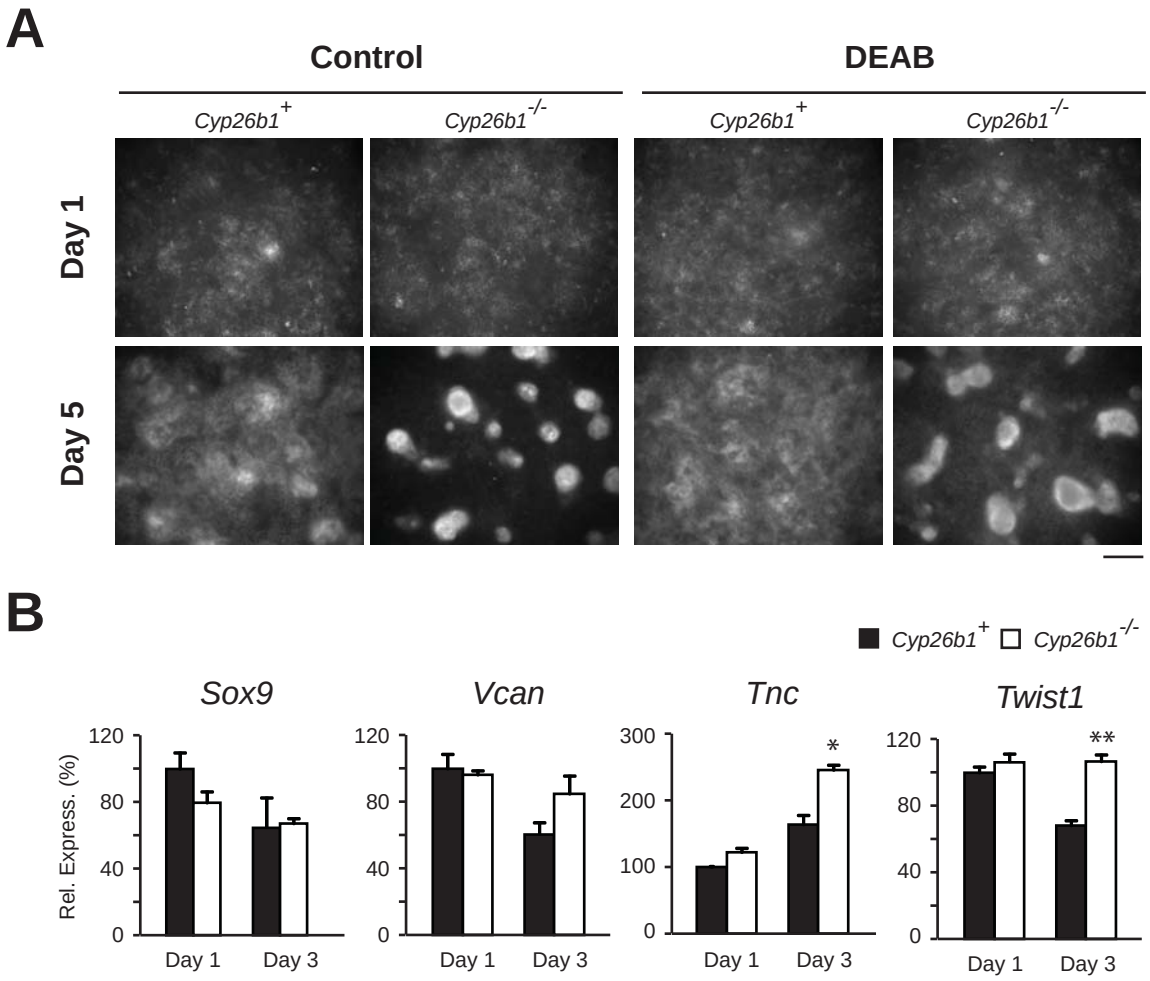
A
Control
DEAB
Cyp26b1+
Cyp26b1-/-
Cyp26b1+
Cyp26b1-/-
Day 1
Day 5
B
Cyp26b1+
Cyp26b1-/-
Sox9
Vcan
Tnc
Twist1
Rel. Express. (%)
120
80
40
0
300
200
100
Day 1
Day 3
*
**

Figure 8. Prechondrogenic cells from *Cyp26b1*$^{-/-}$ animals exhibit reduced differentiation.

A) Alcian blue staining of 4 and 8 day-old PLM cultures with or without DEAB treatment (10μM). B) qPCR analysis of differentiation markers *Sox5*, *Sox6*, *Col2a1*, *Acan*, *Hapln1*, *Comp*, *Mia1*, *Matn1*, and *Cspg4* in PLM cultures after 1 or 3 days of culture. Scale bar, 1mm. Error bars represent 1 s.d. Significance was evaluated in comparison to wildtype controls on the same day and is represented as follows: *$p<0.05$; **$p<0.01$; $^{\#}p<0.001$. nd, 40 cycles of qPCR and transcript not detected.

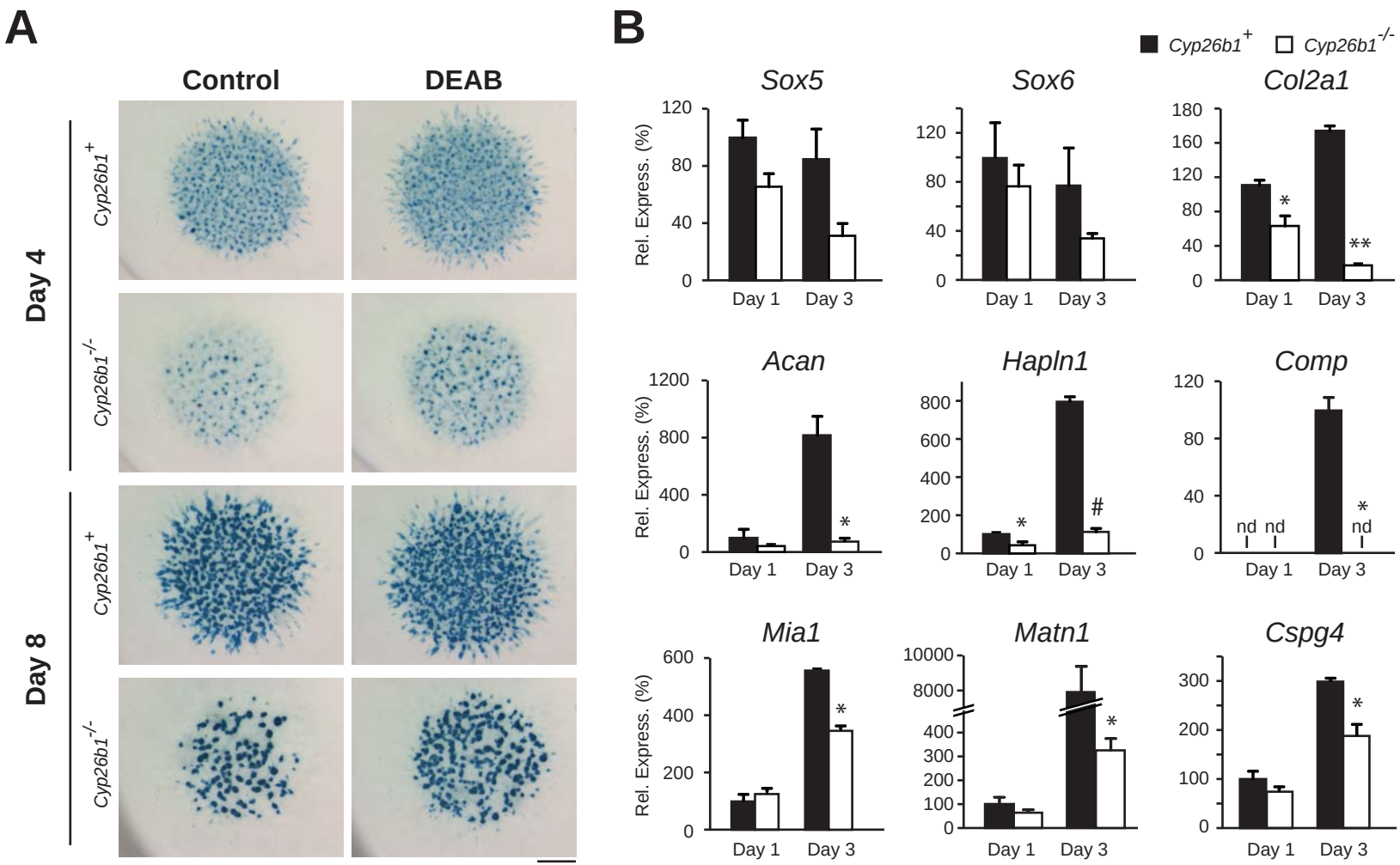
A
Control
DEAB
Day 4
Day 8
Cyp26b1+
Cyp26b1-/-
B
Cyp26b1+
Cyp26b1-/-
Sox5
Sox6
Col2a1
Acan
Hapln1
Comp
Mia1
Matn1
Cspg4
Rel. Express. (%)
Day 1
Day 3
nd
*
**
#

Figure 9. *Cyp26b1*$^{-/-}$ cells exhibit little change in hypertrophy.

A) qPCR analysis of hypertrophic and osteoblast markers *Pthrp*, *Ihh*, *Ptch1*, *Col10a1*, *Runx2*, *Alp1*, *Spp1*, and *Mmp13* in PLM cultures after 1 or 3 days of culture. B) The distribution of MMP13 was evaluated using immunofluorescence. A control with no primary antibody shows that staining is specific for MMP13 expression. For both cultures, the image was taken from the centre of the culture where cartilage nodules are present. Scale bar, 200μm. Error bars represent 1 s.d. Significance was evaluated in comparison to wildtype controls on the same day and is represented as follows: *$p<0.05$; **$p<0.01$; $^{\#}p<0.001$.

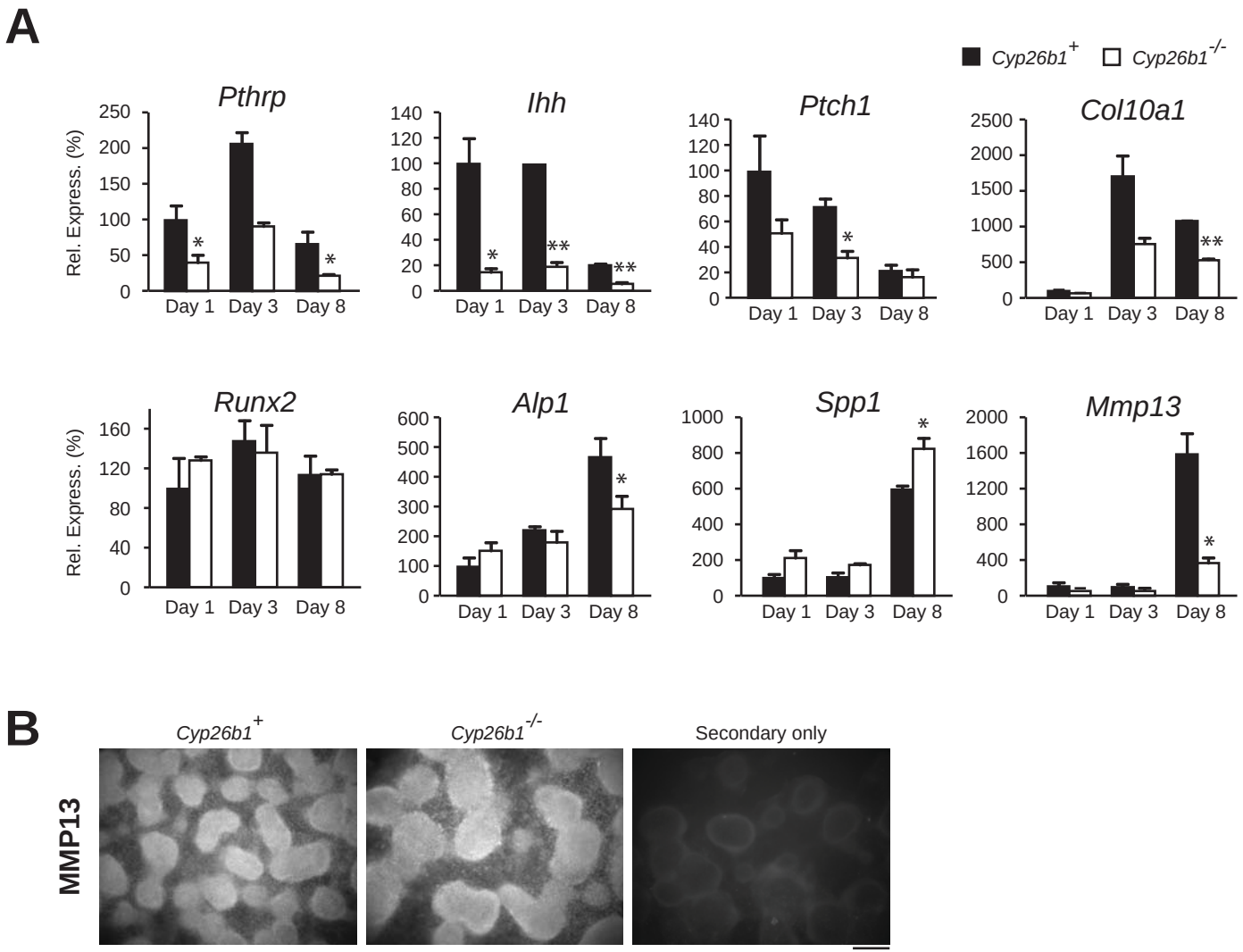
A
Cyp26b1+
Cyp26b1-/-
Pthrp
Ihh
Ptch1
Col10a1
Runx2
Alp1
Spp1
Mmp13
Rel. Expres. (%)
Day 1
Day 3
Day 8
B
MMP13
Cyp26b1+
Cyp26b1-/-
Secondary only

Figure 10. Proximally-derived cells are more sensitive to changes in retinoid signalling. A) Alcian blue staining of 4 and 8 day-old PLM cultures established from the proximal (P) or distal (D) regions of wildtype limbs and treated with ketoconazole (keto, 1µM) or DEAB (10µM). B) Col2-LUC and RARE-LUC reporter activity in PLM cultures derived from P and D limb regions after 1, 3, or 8 days of culture with or without ketoconazole or DEAB treatment. C) qPCR analysis of chondroblast markers in the P and D cell populations after treatment with ketoconzaole or DEAB. RNA was collected after 3 days of culture. Scale bar, 2mm. Error bars represent 1 s.d. Numbers above each bar represent the fold-change from untreated control for each cell population. Significance was evaluated in comparison to untreated proximal or distal controls on the same day and is represented as follows: *$p<0.05$; **$p<0.01$; $^{\#}p<0.001$.

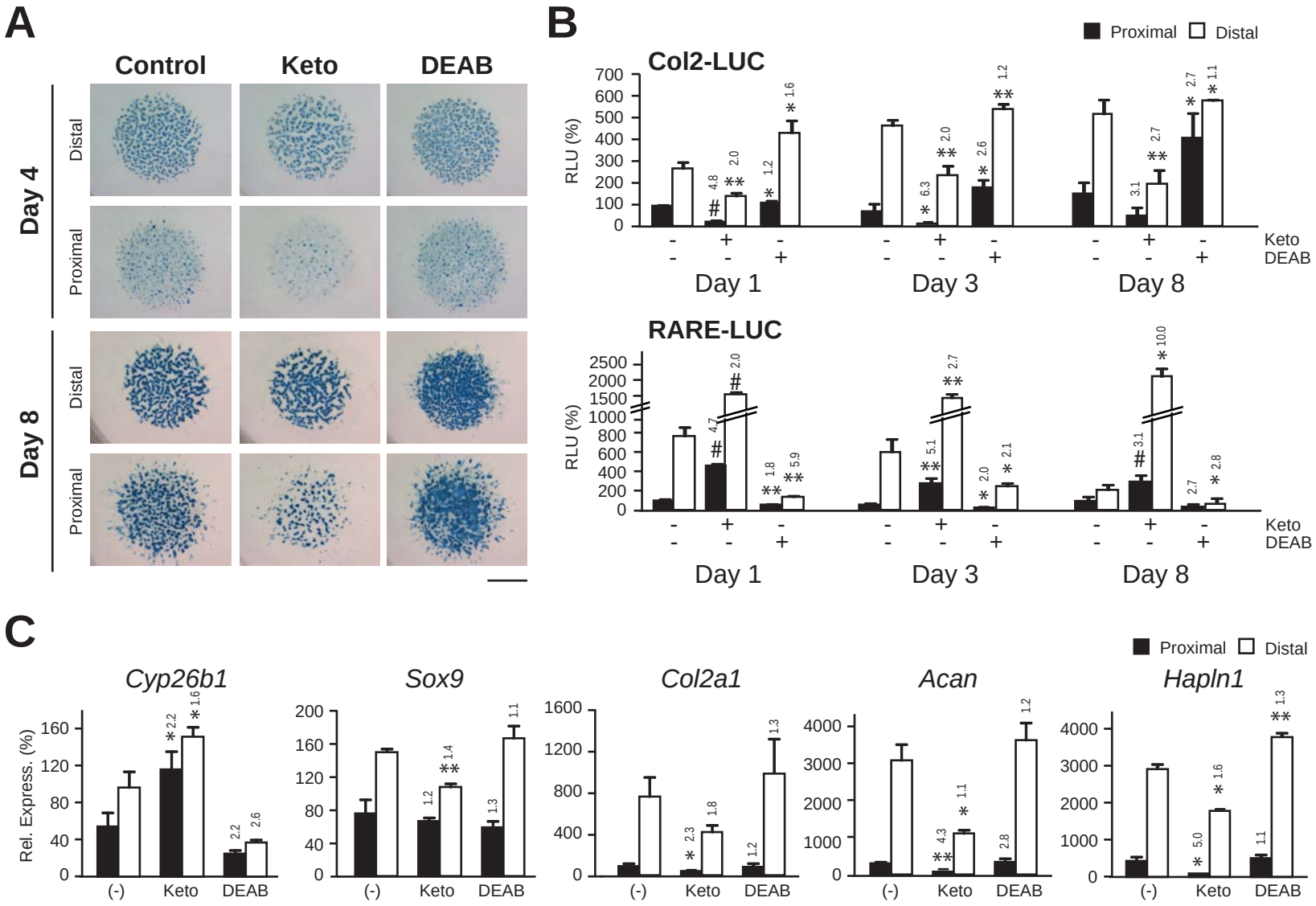
A
Control
Keto
DEAB
Day 4
Day 8
Distal
Proximal
B
Proximal
Distal
Col2-LUC
RLU (%)
Keto
DEAB
Day 1
Day 3
Day 8
RARE-LUC
C
Cyp26b1
Sox9
Col2a1
Acan
Hapln1
Rel. Express. (%)
(-)
Keto
DEAB

Figure 11. Limb mesenchyme from *Cyp26b1*$^{-/-}$ exhibit increases in the expression of tendon markers.

A) qPCR analysis of tendon markers *Scx*, *Tnmd*, and *Col1a1* in PLM cultures derived from wildtype and *Cyp26b1*$^{-/-}$ mice after 1 or 3 days of culture. B) Visualization of EGFP expression in E12.5 *Cyp26b1*$^{+/+}$ and *Cyp26b1*$^{-/-}$ mice expressing the *ScxGFP*$^{+}$ transgene. Scale bar, 1.25mm. C) Visualization of EGFP expression in limbs from E12.5 *Cyp26b1*$^{+/+}$ and *Cyp26b1*$^{-/-}$ mice expressing the *ScxGFP*$^{+}$ transgene. Scale bar, 1.25mm. D) qPCR analysis of *Scx* expression in microdissected limbs from *Cyp26b1*$^{+/+}$ and *Cyp26b1*$^{-/-}$ mice. E) PLM cultures derived from *ScxGFP*$^{+}$ mice were treated with ketoconazole (keto, 1µM) or DEAB (10µM) and EGFP expression was visualized after 1, 3, and 8 days of culture. Scale bar, 200µm. F) qPCR analysis of *Scx* expression in PLM cultures treated with ketoconazole or DEAB and cultured for 1, 3, or 8 days. G) PLM cultures established from *ScxGFP*$^{+}$ mice were treated with Tgfb1 (Tb1, 2 ng/ml), BMP4 (B4, 20 ng/ml), and/or ketoconazole (1µM), and EGFP expression was visualised after 8 days. Scale bar, 200µm. Note that EGFP expression was exposed to different intensities in panels E and G. Error bars represent 1 s.d. Significance was evaluated in comparison to untreated proximal or distal controls from the same day and is represented as follows: *$p<0.05$; **$p<0.01$; $^{\#}p<0.001$.

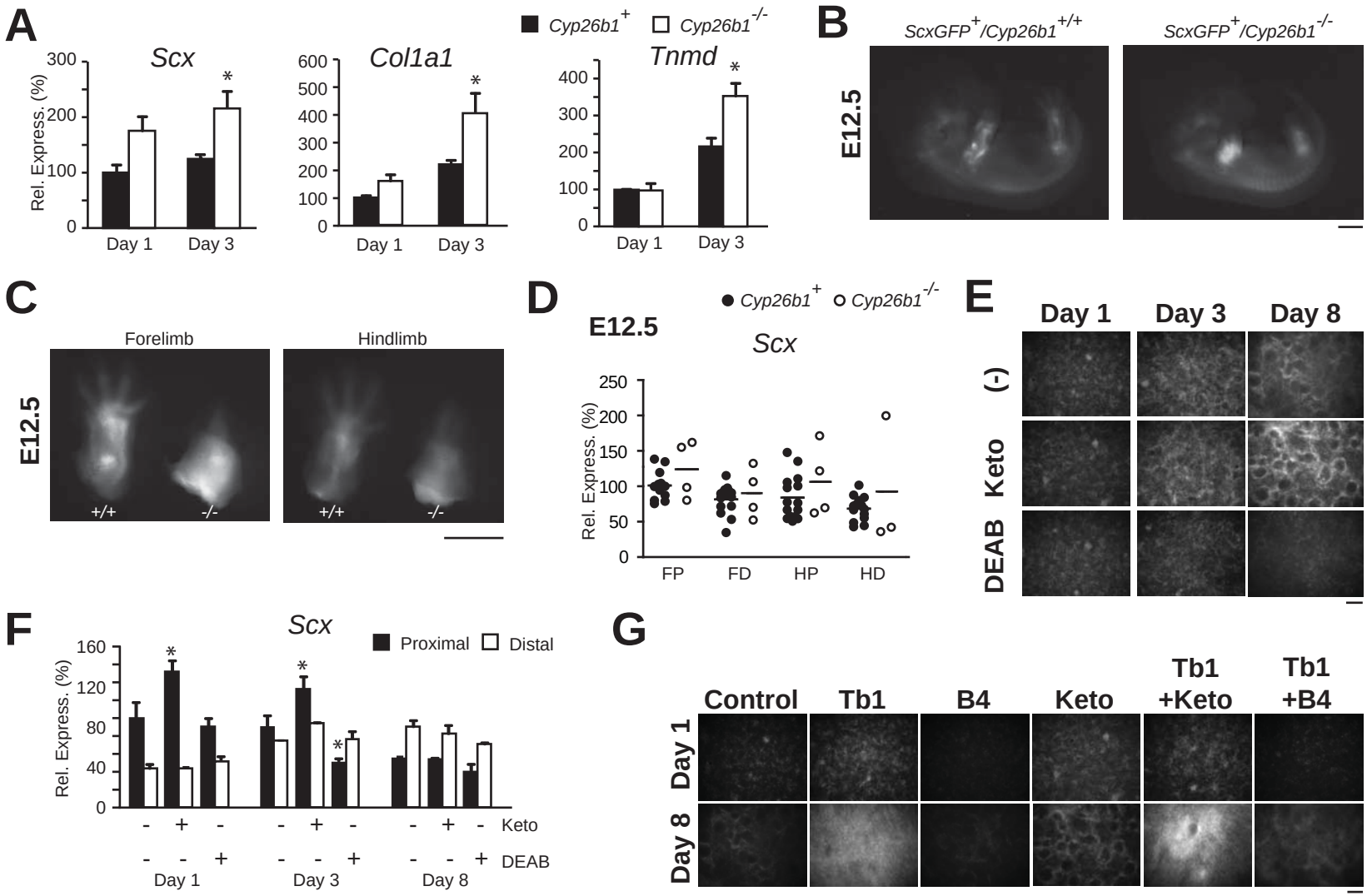
A
Scx
Col1a1
Tnmd
Cyp26b1+
Cyp26b1-/-
Rel. Express. (%)
Day 1
Day 3
B
ScxGFP+/Cyp26b1+/+
ScxGFP+/Cyp26b1-/-
E12.5
C
Forelimb
Hindlimb
+/+
-/-
D
E12.5
Scx
Rel. Express. (%)
FP
FD
HP
HD
E
Day 1
Day 3
Day 8
(-)
Keto
DEAB
F
Scx
Proximal
Distal
Rel. Express. (%)
Keto
DEAB
Day 1
Day 3
Day 8
G
Control
Tb1
B4
Keto
Tb1 +Keto
Tb1 +B4
Day 1
Day 8

CHAPTER 4: DISCUSSION

The limb defects observed in *Cyp26b1*$^{-/-}$ and *Prrx1Cre*$^{+}$*/Cyp26b1*$^{fl/fl}$ mice are characteristic of RA teratogenecity. For many years it has been believed that RA plays an instructive role in limb patterning by acting as a "proximalizing" morphogenetic factor, and that the limb malformations in *Cyp26b1*$^{-/-}$ mice result from a shortening of the proximo-distal axis (Yashiro et al., 2004). However, new evidence suggests that RA is dispensable for early limb patterning, as *Aldh1a2/3* double knockout mice have normal hindlimb development and disruption of Rarg partially rescues the *Cyp26b1*$^{-/-}$ limb phenotype despite altered P-D gene expression (Zhao et al., 2009; Pennimpede et al., 2010b). In this work, we demonstrate that the severity of limb malformations in *Cyp26b1*$^{-/-}$ mice is tightly correlated to levels of retinoid signalling, and that a lack of *Cyp26b1* negatively impacts chondogenesis before the onset of *Ihh* signalling, and positively afterwards. Similar to recent reports on X-irradiation induced phocomelia in chicks, in which the pre-chondrogenic mesenchyme is depleted, the impact of RA on chondrogenesis results in an insufficient number of chondrocytes and subsequent defects in the proper formation of skeletal elements (Galloway et al., 2009). This suggests that the limb phenotype in *Cyp26b1*$^{-/-}$ animals is not due to changes in patterning, but as a result of defects in the execution of a patterning program. In this study, we have used the *Cyp26b1*$^{-/-}$ limb as a model to examine the precise role of endogenous RA signalling in chondrogenesis.

Regulation of chondrogenesis by RA

The first step in the chondrogenic program is the migration of mesenchymal cells from the lateral plate mesoderm to presumptive sites of limb formation, where committed prechondrogenic cells become tightly packed and form precartilaginous condensations (Hall and Miyake, 2000). *Cyp26b1*$^{-/-}$ cells express early condensation markers such as *Sox9*, which is

essential for the commitment of mesenchymal cells towards the chondrogenic lineage, and appear to form condensations. However, *Cyp26b1*$^{-/-}$ cells exhibit a significant decrease in differentiation. Previous studies have demonstrated a requirement for RAR-mediated repression for chondroblast differentiation, and this work demonstrates for the first time that this requirement is also necessary *in vivo* (Weston et al., 2000; Weston et al., 2002). As *Aldh1a2* is expressed in regions that do not form cartilage (Hoffman et al., 2006), it is likely that levels of RA decrease in the centre of condensations where RA cannot diffuse to, allowing some cells to escape the effects of increased RA in *Cyp26b1*$^{-/-}$ condensations and differentiate. Fewer, but much larger, cartilage nodules form, indicating that cells remain and expand in the condensation stage for a long time before their eventual differentiation. Treatment with DEAB is not able to rescue *Cyp26b1*$^{-/-}$ cells, demonstrating that short-term exposure to RA is sufficient to interfere with differentiation. Furthermore, while all limb mesenchyme is very sensitive to changes in endogenous retinoid signalling, proximally-derived cells from the limb, which differentiate before more distal cells, are most affected. Altogether, these results indicate that RA affects prechondrogenic cells at the timing of differentiation and blocks their progression to becoming differentiated chondrocytes.

RA and chondrocyte hypertrophy

Previous studies have demonstrated that retinoids act to promote the transition from prehypertrophy to hypertrophy during endochondral ossification in the developing limb (Koyama et al., 1999). Concurrent with this, we have demonstrated that *Cyp26b1*$^{-/-}$ cells, with the exception of *Ptrhp* and *Ihh*, exhibit modest changes in the expression of hypertrophic-associated markers. The small decrease in *Col10*, *Alp1*, and *Mmp13* expression and the delay in

mineralization likely result from the decrease in chondrogenic differentiation and the formation of fewer, although larger, cartilage nodules.

Growth plates sustain skeletal growth through the proliferation of chondrocytes, matrix synthesis and accumulation, and chondrocyte hypertrophy. The growth plate is divided into two zones, the upper zone which contains immature chondrocytes, maintained by PTHrP signalling, and the lower zone, which contains *Ihh*-expressing prehypertrophic and maturing hypertrophic chondrocytes. PTHrP regulates the expression of *Ihh*, which controls chondrocyte proliferation, and *Ihh* in turn regulates *Pthrp* expression, creating a feedback system that controls the growth of skeletal elements (Kronenberg, 2006). The hypertrophic portions of the growth plate have been shown to contain higher levels of endogenous retinoid signalling than the upper, immature zones and a requirement for RAR-mediated repression in the upper growth plate zone has been shown to maintain chondrocyte function and prevent hypertrophy (Williams et al., 2009; Williams et al., 2010). Previous studies have suggested that RA-mediated repression of target gene expression in the upper zone is necessary to maintain physiologic *Ihh* expression levels (Koyama et al., 1999). We demonstrate in this study that an increase in retinoid signalling substantially decreases *Ihh* expression. Consequently, hypertrophic chondrocytes emerge earlier, with less growth having occurred, and this may partly explain the observed truncation of skeletal elements. The role of RA upstream of *Ihh* is further exemplified by the striking resemblance between *Cyp26b1*$^{-/-}$ and *Ihh*$^{-/-}$ limbs (St-Jacques et al., 1999). Our findings indicate that RA has a negative impact on chondrogenesis before activation of *Ihh* signalling, and a positive impact on chondrocyte hypertrophy.

RA and multipotent mesenchymal cells - cell fate lineage decisions

Multi-potent mesenchymal cells derived from the lateral plate mesoderm have the ability to contribute to lineages such as cartilage, bone, fat, and tendon. We investigated whether *Cyp26b1*$^{-/-}$ cells have the potential to contribute to lineages other than chondogenic, and chose to focus on the tenogenic lineage, with the reasoning that tenocyte differentiation is most closely associated to chondrocyte differentiation. The two lineages share early molecular mechanisms during mesenchyme condensation and close interactions between cartilage and tendon exist during development. An up-regulation of tendon markers was observed in *Cyp26b1*$^{-/-}$ cells, indicating that the decrease in chondrogenesis reflects an increase in commitment to tenogenesis, and potentially other lineages. Notably, cells from the proximally-derived region of the limb were most affected, similar to what was observed with the decrease in chondrogenesis. It is unlikely that functional tenocytes are forming as previous studies have shown that the presence of excess tendon progenitors did not lead to the production of additional or longer tendons, indicating that additional signals are required for the development of a tendon, or because of a reliance on muscle formation (Schweitzer et al., 2001).

It appears that *Cyp26b1*$^{-/-}$ cells maintain the ability to commit to mesenchymal lineages other than chondrogenic. This is not due to the inhibition of cartilage differentiation because treatment with BMP4, which would normally drive chondrocyte differentiation, had little impact. This is consistent with earlier reports that RA is operating downstream of BMPs to impact chondrogenesis (Hoffman et al., 2006). This suggests that RA is actively promoting the maintenance of an undifferentiated progenitor state. It is likely that this is a normal physiological role of RA, as very high levels of retinoids are found in the perichondrium, which is an important source of undifferentiated skeletal precursors during skeletal development,

growth and homeostasis (Koyama et al., 1999). RA is likely maintaining the potential of mesenchymal cells through the up-regulation of both *Twist1* and *Fgf18,* a direct RAR-target gene, both of which repress chondrocyte differentiation, are expressed in the perichondrium, and were found to be significantly elevated in *Cyp26b1*$^{-/-}$ cells (Hinoi et al., 2006; Delacroix et al., 2010). A similar mechanism is observed in the adult and developing forebrain, in which a precursor population of cells in the subventricular zone has been shown to exhibit activated RA signalling (Haskell and LaMantia, 2005). Collectively, these findings highlight an important role for endogenous RA signalling in regulating expression of the chondroblastic phenotype and in maintenance of progenitor cell plasticity (Figure 12).

Figure 12. A model for the role of RA in regulating mesenchymal cell fate during limb development.

Retinoid signalling maintains the potential of mesenchymal cells and inhibits chondroblast differentiation. RA signalling has a negative impact on chondrogenesis before activation of *Ihh* signalling, after which RA signalling has a positive impact on chondrocyte hypertrophy.

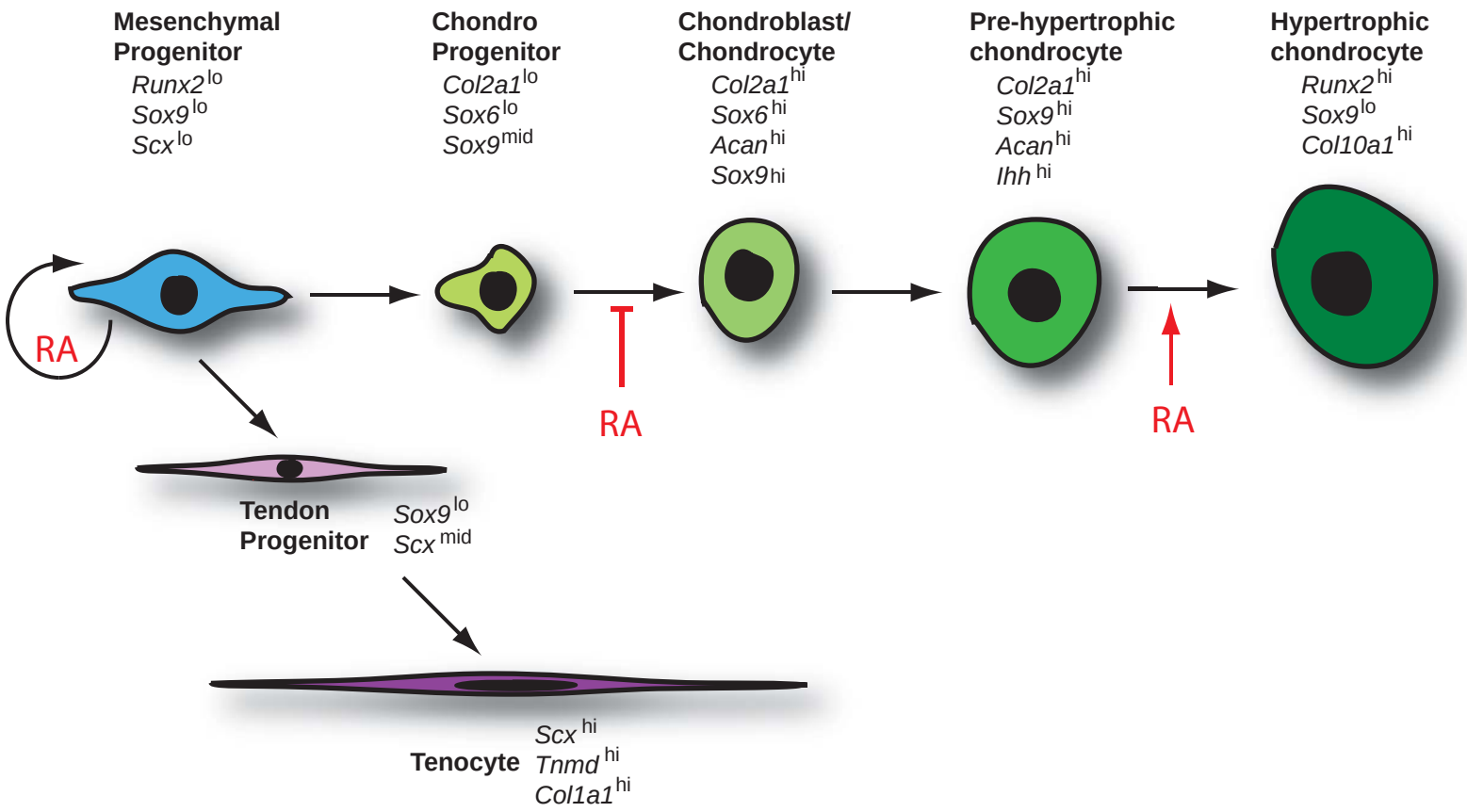
Mesenchymal Progenitor
Runx2 lo
Sox9 lo
Scx lo
Chondro Progenitor
Col2a1 lo
Sox6 lo
Sox9 mid
Chondroblast/ Chondrocyte
Col2a1 hi
Sox6 hi
Acan hi
Sox9 hi
Pre-hypertrophic chondrocyte
Col2a1 hi
Sox9 hi
Acan hi
Ihh hi
Hypertrophic chondrocyte
Runx2 hi
Sox9 lo
Col10a1 hi
RA
RA
RA
Tendon Progenitor
Sox9 lo
Scx mid
Tenocyte
Scx hi
Tnmd hi
Col1a1 hi

CHAPTER 5: CONCLUSION

In this thesis, I have shown that limb defects resulting from increased retinoid signalling are likely due to a defect in the execution of a patterning program, but not in the patterning program per se. Using *Cyp26b1*$^{-/-}$ and *Prrx1Cre*$^{+}$*/Cyp26b1*$^{fl/fl}$ animals, I have shown that limb defects are more severe with increased levels of retinoid signalling, which acts to inhibit chondroblast differentiation. This results in an insufficient number of skeletal precursor cells and defects in the proper formation of skeletal elements. The decrease in chondrogenesis likely reflects the maintenance of an undifferentiated state, and cells appear to have the ability to contribute to several lineages.

Discussion of goals

1. *Generation and characterization of a transgenic mouse with delayed deletion of Cyp26b1:*

   A *Prrx1Cre*$^{+}$*/Cyp26b1*$^{fl/fl}$ mouse, in which *Cyp26b1* is deleted under the direction of the *Prrx1* promoter, was generated. Analysis demonstrated that a very small amount of *Cyp26b1* expression remained at E11.5-12.5. When compared to *Cyp26b1*$^{-/-}$ embryos, RA signalling was increased to a lesser extent, and limb defects were less severe, in *Prrx1Cre*$^{+}$*/Cyp26b1*$^{fl/fl}$ animals.

2. *Investigate the effect of increased RA signalling on different stages of the chondrogenic program*

   PLM cultures were established from wildtype and *Cyp26b1*$^{-/-}$ cells in order to investigate the impact of increased retinoid signalling on the chondrogenic program.

Cyp26b1$^{-/-}$ cells formed prechondrogenic condensations, but exhibited a large decrease in chondroblast differentiation. There was a minimal impact on hypertrophy, which likely resulted from the decrease in chondrocyte differentiation. Cells from the proximal region of the limb bud were more affected by modulation of endogenous retinoid signalling when compared to distally-derived cells. The *in vitro* culture analysis was further validated *in vivo* with qPCR, and a good correlation was found between the two systems.

3. *Determine the mechanism by which increased levels of RA affect skeletal development*

   Cyp26b1$^{-/-}$ cells exhibited an increase in the expression of tendon markers (*Scx*, *Col1a1*, *Tnmd*) both in culture and *in vivo*. Modulation of endogenous retinoid signalling with ketoconazole or DEAB in wildtype micromass cultures also affected the expression of tenocyte markers, and to a greater extent in proximal cultures, where chondrogenesis was found to be most impacted. This indicates that retinoid signalling blocks differentiation and maintains cells in an undifferentiated state with the potential to contribute to multiple lineages.

The research presented in this thesis provides evidence that supports our hypothesis that the limb defects resulting from increased retinoid signalling are due to defects in the execution of a patterning program.

Significance of research

This work is the first to demonstrate that RAR-mediated repression is necessary for chondroblast differentiation *in vivo*, and that retinoid signalling can impact tenocyte fate determination. This research provides a valuable contribution to several fields, most notably:

Developmental biology

This work contributes to the debate on the role of RA in skeletal patterning and provides further evidence that RA is likely dispensable for limb patterning. Importantly, this work re-interprets the mechanisms underlying the limb defects present in *Cyp26b1*$^{-/-}$ mice, which were previously attributed to a shortening of the P-D axis. Additionally, this research contributes to furthering our understanding of how limb morphogenesis is organized and provides insights into the role of RA in cartilage and tendon development.

Cell science

This work contributes to our understanding of the functional potential of cells and the mechanisms that underlie their differentiation. We have demonstrated that the presence of excess RA can affect the development of chondrocytes and tenocytes and this work highlights the role of RA in achieving specific cell fates in the developing limb.

Strengths and limitations

Strengths

This research is technically strong in that it involves a thorough analysis of chondrogenesis at the molecular and cellular level using well-established, accurate, and reliable methods such as the micromass system and encompasses a wide variety of techniques. Several assays were used to demonstrate the same findings; for example, reporter assays, qPCR, and RARE-LacZ analysis was used to analysed activated retinoid signalling, while reporter assays, qPCR, and a variety of cell staining techniques were used to analyse chondrogenesis. Importantly, this work utilizes *in vivo* models (conventional and conditional knockout mice, as well as transgenic GFP expressing mice), which are invaluable to furthering our understanding of the mechanisms that underlie development.

Limitations

There were very few significant limitations while performing this research. One potential weakness is that ketoconazole is not a specific CYP26B1 inhibitor, but also inhibits the activity of CYP26A1 and other P450 enzymes that may be playing a compensatory role in *Cyp26b1*$^{-/-}$ animals. However, ketoconazole has been used in previous studies successfully and was sufficient for my experiments (Hoffman et al., 2006).

It was difficult to properly assess the impact of increased levels of retinoid signalling on hypertrophy as defects in earlier stages of the chondrogenic program affected accurate evaluation of later stages. For example, it was difficult to assess changes in gene expression with confidence when fewer nodules were present in *Cyp26b1*$^{-/-}$ cultures compared to wildtype, as fewer nodules will result in less transcript production. However, this was circumvented by immunostaining of hypertrophic markers, and qualitative comparison of expression levels between the nodules that did form.

Finally, it would be ideal to repeat some of the experiments, such as reporter assays and qPCR, in this thesis with PLM cultures from *Prrx1Cre*$^{+}$*/Cyp26b1*$^{fl/fl}$ mice to demonstrate that a smaller increase in levels of retinoid signalling (compared to *Cyp26b1*$^{-/-}$ mice) results in a greater amount of chondroblast differentiation occurring *in vivo*. It would also be interesting to cross the *Prrx1Cre*$^{+}$*/Cyp26b1*$^{fl/fl}$ mice to *ScxGFP*$^{+}$ mice to visualise *Scx* expression.

Potential applications of research findings

During development, cartilage provides a foundation for most of the skeleton, and elucidating the network of events that underlie chondrogenesis will improve our current understanding of diseases associated with chondrogenic and skeletal abnormalities. In adults, remnants of embryonic cartilage are found at the articular surfaces of bones, and approximately

10% of the Canadian population suffers from osteoarthritis, a disease in which the articular cartilage is destroyed. This causes a reduction in joint mobility and pain, and the regenerative capacity of cartilage is very limited. Many of the reparative processes in the adult involve recapitulation of the embryonic program and therefore a better understanding of how RA regulates cartilage formation will enable the development of treatments aimed at stimulating cartilage repair and/or regeneration in the adult.

Additionally, *Crabp2*, a RA-responsive gene, has been shown to be up-regulated in cases of osteoarthritis and it has been proposed that retinoid signalling may play a central role in osteoarthritis (Davies et al., 2009; Welch et al., 2009). This gives further therapeutic cause for understanding the role of RA in cartilage formation because components of the retinoid signalling pathway may provide potential targets for therapeutic intervention.

The ultimate goal is directed cellular regeneration or repair of damaged and diseased musculoskeletal tissue. The information gained from these studies will aid our understanding of the basic processes that regulate cartilage and tendon formation. This will impact efforts to enhance repair and also in directing the differentiation of multi-potential progenitor or stem cells towards a chondrocyte or tenocyte fate for cartilage and tendon repair.

Future research directions

There are several different directions for future work. Firstly, the expression of patterning genes was not addressed in theses studies. Determining whether segment specification is altered between *Prrx1Cre*$^{+}$*/Cyp26b1*$^{fl/fl}$ and *Cyp26b1*$^{-/-}$ mice, despite the difference in severity of limb defects, would provide further insights as to the role of RA in limb patterning. In future experiments, *in situ* hybridization and qPCR could be used to examine the

expression of markers such as *Meis1*, *Meis2* and *Shox2* (stylopod), *Hoxa11* (zeugopod), and *Hoxa13* and *Hoxd13* (autopod).

Another potential line of work could be focused on examining the role of RA in tenogenesis. Very little is known about the molecular mechanisms that underlie tenogenesis, and we have demonstrated for the first time that the anti-chondrogenic properties of RA reflect a positive effect on tenocyte differentiation. Future experiments would focus on elucidating the role of retinoid signalling in tenocyte formation – whether RA is promoting a fully developed tenocyte fate, or simply maintaining mesenchymal cells in an undifferentiated state with the potential to contribute to multiple lineages. Additionally, future experiments could examine the impact on other lineages such as osteogenic and adipogenic.

The role of RA in skeletogenesis could be further examined by generating a temporal knockout of *Cyp26b1* to assess the role of *Cyp26b1* at later stages in development. By crossing *Cyp26b1*$^{fl/fl}$ mice to *Rosa26*CreERT2 transgenic mice, *Cyp26b1* can be deleted at any time with tamoxifen injections that activate Cre recombinase. This could be performed at E10-11, when patterning has been specified, in order to validate that RA is dispensable for patterning, or to properly assess the impact of a lack of *Cyp26b1* expression on hypertrophy after differentiation has occurred. In addition, conditional deletion of *Cyp26b1* using transgenic *Col2*- and *Col10*-Cre expressing mice would allow for analysis of the role of *Cyp26b1* before and after hypertrophy, respectively. As *Cyp26b1*$^{-/-}$ mice are embryonic lethal, generation of these conditional knockout mouse strains would be crucial to evaluate of the role of *Cyp26b1* in adult bone metabolism.

Finally, another transgenic mouse that would provide valuable insights as to the role of RA signalling in skeletogenesis, is a *Cyp26b1* over-expression transgenic. I predict that this

mouse would present with increased cartilage formation and ectopic cartilage in the limb, and characterizing the phenotype of a *Cyp26b1* over-expressing mouse would compliment the loss-of-function approach already taken. This would allow us to directly test the effect of a deficiency of RA in chondrogenesis. Ultimately, identification of the downstream targets of retinoid signalling, using both *Cyp26b1* knockout and over-expression transgenic mice, will provide insights as to the role of retinoid signalling in chondrogenesis and skeletal development.

REFERENCES

Abu-Abed S, Dolle P, Metzger D, Beckett B, Chambon P, Petkovich M. 2001. The retinoic acid-metabolizing enzyme, CYP26A1, is essential for normal hindbrain patterning, vertebral identity, and development of posterior structures. Genes Dev 15:226-240.

Abu-Abed S, MacLean G, Fraulob V, Chambon P, Petkovich M, Dolle P. 2002. Differential expression of the retinoic acid-metabolizing enzymes CYP26A1 and CYP26B1 during murine organogenesis. Mech Dev 110:173-177.

Adams CS, Shapiro IM. 2002. The fate of the terminally differentiated chondrocyte: evidence for microenvironmental regulation of chondrocyte apoptosis. Crit Rev Oral Biol Med 13:465-473.

Ahrens PB, Solursh M, Reiter RS. 1977. Stage-related capacity for limb chondrogenesis in cell culture. Dev Biol 60:69-82.

Akiyama H, Chaboissier MC, Martin JF, Schedl A, de Crombrugghe B. 2002. The transcription factor Sox9 has essential roles in successive steps of the chondrocyte differentiation pathway and is required for expression of Sox5 and Sox6. Genes Dev 16:2813-2828.

Akiyama H, Kim JE, Nakashima K, Balmes G, Iwai N, Deng JM, Zhang Z, Martin JF, Behringer RR, Nakamura T, de Crombrugghe B. 2005. Osteo-chondroprogenitor cells are derived from Sox9 expressing precursors. Proc Natl Acad Sci U S A 102:14665-14670.

Asou Y, Nifuji A, Tsuji K, Shinomiya K, Olson EN, Koopman P, Noda M. 2002. Coordinated expression of scleraxis and Sox9 genes during embryonic development of tendons and cartilage. J Orthop Res 20:827-833.

Barna M, Niswander L. 2007. Visualization of cartilage formation: insight into cellular properties of skeletal progenitors and chondrodysplasia syndromes. Dev Cell 12:931-941.

Bell DM, Leung KK, Wheatley SC, Ng LJ, Zhou S, Ling KW, Sham MH, Koopman P, Tam PP, Cheah KS. 1997. SOX9 directly regulates the type-II collagen gene. Nat Genet 16:174-178.

Brockes JP. 1997. Amphibian limb regeneration: rebuilding a complex structure. Science 276:81-87.

Cash DE, Bock CB, Schughart K, Linney E, Underhill TM. 1997. Retinoic acid receptor alpha function in vertebrate limb skeletogenesis: a modulator of chondrogenesis. J Cell Biol 136:445-457.

Colnot C, de la Fuente L, Huang S, Hu D, Lu C, St-Jacques B, Helms JA. 2005. Indian hedgehog synchronizes skeletal angiogenesis and perichondrial maturation with cartilage development. Development 132:1057-1067.

Colnot CI, Helms JA. 2001. A molecular analysis of matrix remodeling and angiogenesis during long bone development. Mech Dev 100:245-250.

Crawford K, Stocum DL. 1988. Retinoic acid coordinately proximalizes regenerate pattern and blastema differential affinity in axolotl limbs. Development 102:687-698.

Davies MR, Ribeiro LR, Downey-Jones M, Needham MR, Oakley C, Wardale J. 2009. Ligands for retinoic acid receptors are elevated in osteoarthritis and may contribute to pathologic processes in the osteoarthritic joint. Arthritis Rheum 60:1722-1732.

De Crombrugghe B, Akiyama H, editors. 2009. Transcriptional control of chondrocyte differentiation. Cold Spring Harbour: Cold Spring Harbour Laboratory Press. 147-170 pp.

de Crombrugghe B, Lefebvre V, Behringer RR, Bi W, Murakami S, Huang W. 2000. Transcriptional mechanisms of chondrocyte differentiation. Matrix Biol 19:389-394.

Delacroix L, Moutier E, Altobelli G, Legras S, Poch O, Choukrallah MA, Bertin I, Jost B, Davidson I. 2010. Cell-specific interaction of retinoic acid receptors with target genes in mouse embryonic fibroblasts and embryonic stem cells. Mol Cell Biol 30:231-244.

DeLise AM, Fischer L, Tuan RS. 2000. Cellular interactions and signaling in cartilage development. Osteoarthritis Cartilage 8:309-334.

Docheva D, Hunziker EB, Fassler R, Brandau O. 2005. Tenomodulin is necessary for tenocyte proliferation and tendon maturation. Mol Cell Biol 25:699-705.

Duester G. 2008. Retinoic acid synthesis and signaling during early organogenesis. Cell 134:921-931.

Dupe V, Ghyselinck NB, Thomazy V, Nagy L, Davies PJ, Chambon P, Mark M. 1999. Essential roles of retinoic acid signaling in interdigital apoptosis and control of BMP-7 expression in mouse autopods. Dev Biol 208:30-43.

Ede D, editor. 1983. Cellular condensations and chondrogenesis. New York: Academic Press. 143-185 pp.

Fujii H, Sato T, Kaneko S, Gotoh O, Fujii-Kuriyama Y, Osawa K, Kato S, Hamada H. 1997. Metabolic inactivation of retinoic acid by a novel P450 differentially expressed in developing mouse embryos. EMBO J 16:4163-4173.

Galloway JL, Delgado I, Ros MA, Tabin CJ. 2009. A reevaluation of X-irradiation-induced phocomelia and proximodistal limb patterning. Nature 460:400-404.

Germain P, Chambon P, Eichele G, Evans RM, Lazar MA, Leid M, De Lera AR, Lotan R, Mangelsdorf DJ, Gronemeyer H. 2006. International Union of Pharmacology. LX. Retinoic acid receptors. Pharmacol Rev 58:712-725.

Gibert Y, Gajewski A, Meyer A, Begemann G. 2006. Induction and prepatterning of the zebrafish pectoral fin bud requires axial retinoic acid signaling. Development 133:2649-2659.

Hall BK, Miyake T. 1992. The membranous skeleton: the role of cell condensations in vertebrate skeletogenesis. Anat Embryol (Berl) 186:107-124.

Hall BK, Miyake T. 2000. All for one and one for all: condensations and the initiation of skeletal development. Bioessays 22:138-147.

Haskell GT, LaMantia AS. 2005. Retinoic acid signaling identifies a distinct precursor population in the developing and adult forebrain. J Neurosci 25:7636-7647.

Healy C, Uwanogho D, Sharpe PT. 1996. Expression of the chicken Sox9 gene marks the onset of cartilage differentiation. Ann N Y Acad Sci 785:261-262.

Healy C, Uwanogho D, Sharpe PT. 1999. Regulation and role of Sox9 in cartilage formation. Dev Dyn 215:69-78.

Helms JA, Kim CH, Eichele G, Thaller C. 1996. Retinoic acid signaling is required during early chick limb development. Development 122:1385-1394.

Hinoi E, Bialek P, Chen YT, Rached MT, Groner Y, Behringer RR, Ornitz DM, Karsenty G. 2006. Runx2 inhibits chondrocyte proliferation and hypertrophy through its expression in the perichondrium. Genes Dev 20:2937-2942.

Hoffman LM, Garcha K, Karamboulas K, Cowan MF, Drysdale LM, Horton WA, Underhill TM. 2006. BMP action in skeletogenesis involves attenuation of retinoid signaling. J Cell Biol 174:101-113.

Ikeda T, Kamekura S, Mabuchi A, Kou I, Seki S, Takato T, Nakamura K, Kawaguchi H, Ikegawa S, Chung UI. 2004. The combination of SOX5, SOX6, and SOX9 (the SOX trio) provides signals sufficient for induction of permanent cartilage. Arthritis Rheum 50:3561-3573.

Ito Y, Toriuchi N, Yoshitaka T, Ueno-Kudoh H, Sato T, Yokoyama S, Nishida K, Akimoto T, Takahashi M, Miyaki S, Asahara H. 2010. The Mohawk homeobox gene is a critical regulator of tendon differentiation. Proc Natl Acad Sci U S A 107:10538-10542.

Kalter H, Warkany J. 1961. Experimental production of congenital malformations in strains of inbred mice by maternal treatment with hypervitaminosis A. Am J Pathol 38:1-21.

Karamboulas K, Dranse HJ, Underhill TM. 2010. Regulation of BMP-dependent chondrogenesis in early limb mesenchyme by TGFbeta signals. J Cell Sci 123:2068-2076.

Kimura A, Inose H, Yano F, Fujita K, Ikeda T, Sato S, Iwasaki M, Jinno T, Ae K, Fukumoto S, Takeuchi Y, Itoh H, Imamura T, Kawaguchi H, Chung UI, Martin JF, Iseki S, Shinomiya K, Takeda S. 2010. Runx1 and Runx2 cooperate during sternal morphogenesis. Development 137:1159-1167.

Koyama E, Golden EB, Kirsch T, Adams SL, Chandraratna RA, Michaille JJ, Pacifici M. 1999. Retinoid signaling is required for chondrocyte maturation and endochondral bone formation during limb skeletogenesis. Dev Biol 208:375-391.

Kronenberg HM. 2006. PTHrP and skeletal development. Ann N Y Acad Sci 1068:1-13.

Kronenberg HM, McMahon AP, Tabin C, editors. 2009. Growth Factors and Chondrogenesis. Cold Spring Harbour: Cold Spring Harbour University Press.

Kwasigroch TE, Kochhar DM. 1980. Production of congenital limb defects with retinoic acid: phenomenological evidence of progressive differentiation during limb morphogenesis. Anat Embryol (Berl) 161:105-113.

Lammer EJ, Chen DT, Hoar RM, Agnish ND, Benke PJ, Braun JT, Curry CJ, Fernhoff PM, Grix AW, Jr., Lott IT, et al. 1985. Retinoic acid embryopathy. N Engl J Med 313:837-841.

Lefebvre V. 2002. Toward understanding the functions of the two highly related Sox5 and Sox6 genes. J Bone Miner Metab 20:121-130.

Lefebvre V, Huang W, Harley VR, Goodfellow PN, de Crombrugghe B. 1997. SOX9 is a potent activator of the chondrocyte-specific enhancer of the pro alpha1(II) collagen gene. Mol Cell Biol 17:2336-2346.

Lefebvre V, Li P, de Crombrugghe B. 1998. A new long form of Sox5 (L-Sox5), Sox6 and Sox9 are coexpressed in chondrogenesis and cooperatively activate the type II collagen gene. EMBO J 17:5718-5733.

Lefebvre V, Smits P. 2005. Transcriptional control of chondrocyte fate and differentiation. Birth Defects Res C Embryo Today 75:200-212.

Lewandoski M, Mackem S. 2009. Limb development: the rise and fall of retinoic acid. Curr Biol 19:R558-561.

Logan M, Martin JF, Nagy A, Lobe C, Olson EN, Tabin CJ. 2002. Expression of Cre Recombinase in the developing mouse limb bud driven by a Prxl enhancer. Genesis 33:77-80.

Lohnes D, Mark M, Mendelsohn C, Dolle P, Dierich A, Gorry P, Gansmuller A, Chambon P. 1994. Function of the retinoic acid receptors (RARs) during development (I). Craniofacial and skeletal abnormalities in RAR double mutants. Development 120:2723-2748.

MacLean G, Abu-Abed S, Dolle P, Tahayato A, Chambon P, Petkovich M. 2001. Cloning of a novel retinoic-acid metabolizing cytochrome P450, Cyp26B1, and comparative expression analysis with Cyp26A1 during early murine development. Mech Dev 107:195-201.

Maclean G, Dolle P, Petkovich M. 2009. Genetic disruption of CYP26B1 severely affects development of neural crest derived head structures, but does not compromise hindbrain patterning. Dev Dyn 238:732-745.

MacLean G, Li H, Metzger D, Chambon P, Petkovich M. 2007. Apoptotic extinction of germ cells in testes of Cyp26b1 knockout mice. Endocrinology 148:4560-4567.

Maden M. 1982. Vitamin A and pattern formation in the regenerating limb. Nature 295:672-675.

Maes C, Kobayashi T, Selig MK, Torrekens S, Roth SI, Mackem S, Carmeliet G, Kronenberg HM. 2010. Osteoblast precursors, but not mature osteoblasts, move into developing and fractured bones along with invading blood vessels. Dev Cell 19:329-344.

Mark M, Ghyselinck NB, Chambon P. 2006. Function of retinoid nuclear receptors: lessons from genetic and pharmacological dissections of the retinoic acid signaling pathway during mouse embryogenesis. Annu Rev Pharmacol Toxicol 46:451-480.

Mark M, Ghyselinck NB, Chambon P. 2009. Function of retinoic acid receptors during embryonic development. Nucl Recept Signal 7:e002.

McLeod MJ. 1980. Differential staining of cartilage and bone in whole mouse fetuses by alcian blue and alizarin red S. Teratology 22:299-301.

Mercader N, Leonardo E, Piedra ME, Martinez AC, Ros MA, Torres M. 2000. Opposing RA and FGF signals control proximodistal vertebrate limb development through regulation of Meis genes. Development 127:3961-3970.

Mic FA, Haselbeck RJ, Cuenca AE, Duester G. 2002. Novel retinoic acid generating activities in the neural tube and heart identified by conditional rescue of Raldh2 null mutant mice. Development 129:2271-2282.

Mic FA, Sirbu IO, Duester G. 2004. Retinoic acid synthesis controlled by Raldh2 is required early for limb bud initiation and then later as a proximodistal signal during apical ectodermal ridge formation. J Biol Chem 279:26698-26706.

Mollard R, Viville S, Ward SJ, Decimo D, Chambon P, Dolle P. 2000. Tissue-specific expression of retinoic acid receptor isoform transcripts in the mouse embryo. Mech Dev 94:223-232.

Muramatsu S, Wakabayashi M, Ohno T, Amano K, Ooishi R, Sugahara T, Shiojiri S, Tashiro K, Suzuki Y, Nishimura R, Kuhara S, Sugano S, Yoneda T, Matsuda A. 2007. Functional gene screening system identified TRPV4 as a regulator of chondrogenic differentiation. J Biol Chem 282:32158-32167.

Niederreither K, Dolle P. 2008. Retinoic acid in development: towards an integrated view. Nat Rev Genet 9:541-553.

Niederreither K, Subbarayan V, Dolle P, Chambon P. 1999. Embryonic retinoic acid synthesis is essential for early mouse post-implantation development. Nat Genet 21:444-448.

Niederreither K, Vermot J, Messaddeq N, Schuhbaur B, Chambon P, Dolle P. 2001. Embryonic retinoic acid synthesis is essential for heart morphogenesis in the mouse. Development 128:1019-1031.

Niederreither K, Vermot J, Schuhbaur B, Chambon P, Dolle P. 2000. Retinoic acid synthesis and hindbrain patterning in the mouse embryo. Development 127:75-85.

Niswander L. 2003. Pattern formation: old models out on a limb. Nat Rev Genet 4:133-143.

Niswander L, Tickle C, Vogel A, Booth I, Martin GR. 1993. FGF-4 replaces the apical ectodermal ridge and directs outgrowth and patterning of the limb. Cell 75:579-587.

Okazaki K, Sandell LJ. 2004. Extracellular matrix gene regulation. Clin Orthop Relat Res:S123-128.

Olsen BR, Reginato AM, Wang W. 2000. Bone development. Annu Rev Cell Dev Biol 16:191-220.

Parr BA, McMahon AP. 1995. Dorsalizing signal Wnt-7a required for normal polarity of D-V and A-P axes of mouse limb. Nature 374:350-353.

Pearse RV, 2nd, Scherz PJ, Campbell JK, Tabin CJ. 2007. A cellular lineage analysis of the chick limb bud. Dev Biol 310:388-400.

Pennimpede T, Cameron DA, Maclean GA, Li H, Abu-Abed S, Petkovich M. 2010a. The role of CYP26 enzymes in defining appropriate retinoic acid exposure during embryogenesis. Birth Defects Res A Clin Mol Teratol.

Pennimpede T, Cameron DA, MacLean GA, Petkovich M. 2010b. Analysis of Cyp26b1/Rarg compound-null mice reveals two genetically separable effects of retinoic acid on limb outgrowth. Dev Biol 339:179-186.

Pogue R, Lyons K. 2006. BMP signaling in the cartilage growth plate. Curr Top Dev Biol 76:1-48.

Pryce BA, Brent AE, Murchison ND, Tabin CJ, Schweitzer R. 2007. Generation of transgenic tendon reporters, ScxGFP and ScxAP, using regulatory elements of the scleraxis gene. Dev Dyn 236:1677-1682.

Pryce BA, Watson SS, Murchison ND, Staverosky JA, Dunker N, Schweitzer R. 2009. Recruitment and maintenance of tendon progenitors by TGFbeta signaling are essential for tendon formation. Development 136:1351-1361.

Ray WJ, Bain G, Yao M, Gottlieb DI. 1997. CYP26, a novel mammalian cytochrome P450, is induced by retinoic acid and defines a new family. J Biol Chem 272:18702-18708.

Reinhold MI, Kapadia RM, Liao Z, Naski MC. 2006. The Wnt-inducible transcription factor Twist1 inhibits chondrogenesis. J Biol Chem 281:1381-1388.

Riddle RD, Johnson RL, Laufer E, Tabin C. 1993. Sonic hedgehog mediates the polarizing activity of the ZPA. Cell 75:1401-1416.

Ross SA, McCaffery PJ, Drager UC, De Luca LM. 2000. Retinoids in embryonal development. Physiol Rev 80:1021-1054.

Rossant J, Zirngibl R, Cado D, Shago M, Giguere V. 1991. Expression of a retinoic acid response element-hsplacZ transgene defines specific domains of transcriptional activity during mouse embryogenesis. Genes Dev 5:1333-1344.

Saunders JW, Jr. 1948. The proximo-distal sequence of origin of the parts of the chick wing and the role of the ectoderm. J Exp Zool 108:363-403.

Schweitzer R, Chyung JH, Murtaugh LC, Brent AE, Rosen V, Olson EN, Lassar A, Tabin CJ. 2001. Analysis of the tendon cell fate using Scleraxis, a specific marker for tendons and ligaments. Development 128:3855-3866.

Scott A, Sampaio A, Abraham T, Duronio C, Underhill TM. 2010. Scleraxis expression is coordinately regulated in a murine model of patellar tendon injury. J Orthop Res.

Sessler RJ, Noy N. 2005. A ligand-activated nuclear localization signal in cellular retinoic acid binding protein-II. Mol Cell 18:343-353.

Shenefelt RE. 1972. Morphogenesis of malformations in hamsters caused by retinoic acid: relation to dose and stage at treatment. Teratology 5:103-118.

Soeda T, Deng JM, de Crombrugghe B, Behringer RR, Nakamura T, Akiyama H. 2010. Sox9-expressing precursors are the cellular origin of the cruciate ligament of the knee joint and the limb tendons. Genesis.

Solursh M, editor. 1983. Cell-cell interactions and chondrogenesis. New York: Academic Press. 121-141 pp.

St-Jacques B, Hammerschmidt M, McMahon AP. 1999. Indian hedgehog signaling regulates proliferation and differentiation of chondrocytes and is essential for bone formation. Genes Dev 13:2072-2086.

Stratford T, Horton C, Maden M. 1996. Retinoic acid is required for the initiation of outgrowth in the chick limb bud. Curr Biol 6:1124-1133.

Summerbell D, Lewis JH, Wolpert L. 1973. Positional information in chick limb morphogenesis. Nature 244:492-496.

Tabin C, Wolpert L. 2007. Rethinking the proximodistal axis of the vertebrate limb in the molecular era. Genes Dev 21:1433-1442.

Tahayato A, Dolle P, Petkovich M. 2003. Cyp26C1 encodes a novel retinoic acid-metabolizing enzyme expressed in the hindbrain, inner ear, first branchial arch and tooth buds during murine development. Gene Expr Patterns 3:449-454.

Uehara M, Yashiro K, Mamiya S, Nishino J, Chambon P, Dolle P, Sakai Y. 2007. CYP26A1 and CYP26C1 cooperatively regulate anterior-posterior patterning of the developing brain and the production of migratory cranial neural crest cells in the mouse. Dev Biol 302:399-411.

Underhill TM, Weston AD. 1998. Retinoids and their receptors in skeletal development. Microsc Res Tech 43:137-155.

Welch ID, Cowan MF, Beier F, Underhill TM. 2009. The retinoic acid binding protein CRABP2 is increased in murine models of degenerative joint disease. Arthritis Res Ther 11:R14.

Weston AD, Chandraratna RA, Torchia J, Underhill TM. 2002. Requirement for RAR-mediated gene repression in skeletal progenitor differentiation. J Cell Biol 158:39-51.

Weston AD, Hoffman LM, Underhill TM. 2003. Revisiting the role of retinoid signaling in skeletal development. Birth Defects Res C Embryo Today 69:156-173.

Weston AD, Rosen V, Chandraratna RA, Underhill TM. 2000. Regulation of skeletal progenitor differentiation by the BMP and retinoid signaling pathways. J Cell Biol 148:679-690.

White JA, Guo YD, Baetz K, Beckett-Jones B, Bonasoro J, Hsu KE, Dilworth FJ, Jones G, Petkovich M. 1996. Identification of the retinoic acid-inducible all-trans-retinoic acid 4-hydroxylase. J Biol Chem 271:29922-29927.

Williams JA, Kane M, Okabe T, Enomoto-Iwamoto M, Napoli JL, Pacifici M, Iwamoto M. 2010. Endogenous retinoids in mammalian growth plate cartilage: analysis and roles in matrix homeostasis and turnover. J Biol Chem.

Williams JA, Kondo N, Okabe T, Takeshita N, Pilchak DM, Koyama E, Ochiai T, Jensen D, Chu ML, Kane MA, Napoli JL, Enomoto-Iwamoto M, Ghyselinck N, Chambon P, Pacifici M, Iwamoto M. 2009. Retinoic acid receptors are required for skeletal growth, matrix homeostasis and growth plate function in postnatal mouse. Dev Biol 328:315-327.

Wright E, Hargrave MR, Christiansen J, Cooper L, Kun J, Evans T, Gangadharan U, Greenfield A, Koopman P. 1995. The Sry-related gene Sox9 is expressed during chondrogenesis in mouse embryos. Nat Genet 9:15-20.

Wu X, Shi W, Cao X. 2007. Multiplicity of BMP signaling in skeletal development. Ann N Y Acad Sci 1116:29-49.

Xie WF, Zhang X, Sakano S, Lefebvre V, Sandell LJ. 1999. Trans-activation of the mouse cartilage-derived retinoic acid-sensitive protein gene by Sox9. J Bone Miner Res 14:757-763.

Xu PX, Cheng J, Epstein JA, Maas RL. 1997. Mouse Eya genes are expressed during limb tendon development and encode a transcriptional activation function. Proc Natl Acad Sci U S A 94:11974-11979.

Yashiro K, Zhao X, Uehara M, Yamashita K, Nishijima M, Nishino J, Saijoh Y, Sakai Y, Hamada H. 2004. Regulation of retinoic acid distribution is required for proximodistal patterning and outgrowth of the developing mouse limb. Dev Cell 6:411-422.

Yoon BS, Lyons KM. 2004. Multiple functions of BMPs in chondrogenesis. J Cell Biochem 93:93-103.

Zhao X, Sirbu IO, Mic FA, Molotkova N, Molotkov A, Kumar S, Duester G. 2009. Retinoic acid promotes limb induction through effects on body axis extension but is unnecessary for limb patterning. Curr Biol 19:1050-1057.

APPENDIX

The appendix contains supplemental figures.

Figure A1. Additional analysis of *Cyp26b1* transgenic mice.

A) Alcian blue and alizarin red skeletal staining of E18.5 *Cyp26b1*$^{+/+}$ and *Prrx1Cre*$^{-}$*/Cyp26b1*$^{fl/fl}$ embryos demonstrates that there is no difference between wildtype controls in the two transgenic mouse lines. Scale bar, 25mm. B) X-gal staining of E11.5 and E13.5 limbs from wildtype and *Cyp26b1*$^{-/-}$ mice expressing the RARE-LacZ transgene. Scale bar, 2mm. C) qPCR analysis of *Cyp26b1* and *Rarb* expression in forelimb proximal (FP) and distal (FD) and hindlimb proximal (HP) and distal (HD) regions from E11.5 limbs. Single embryos were analyzed and repeated with similar results. D) qPCR analysis of *Cyp26b1*, *Crabp2*, *Fgf18*, *Pthr1*, and *Vegfa* expression in PLM cultures after 1, 3, or 8 days of culture. Error bars represent 1 s.d. Significance was evaluated in comparison to wildtype controls on the same day and is represented as follows: *$p<0.05$; **$p<0.01$; $^{\#}p<0.001$. nd, 40 cycles of qPCR and transcript not detected.

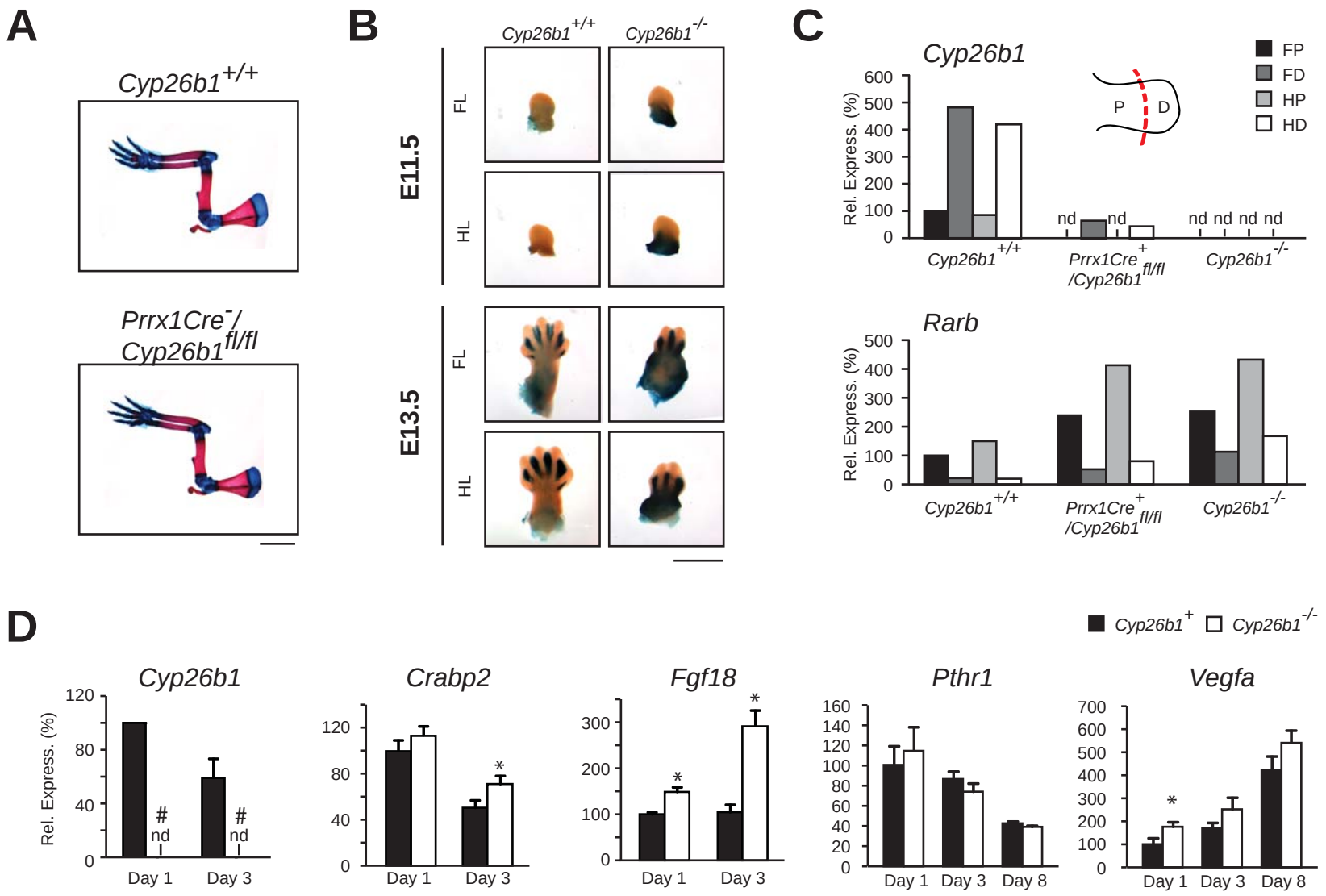
A
Cyp26b1+/+
Prrx1Cre-/
Cyp26b1fl/fl
B
Cyp26b1+/+
Cyp26b1-/-
E11.5
E13.5
FL
HL
C
Cyp26b1
FP
FD
HP
HD
Rel. Express. (%)
P
D
nd
Cyp26b1+/+
Prrx1Cre+
/Cyp26b1fl/fl
Cyp26b1-/-
Rarb
D
Cyp26b1+
Cyp26b1-/-
Cyp26b1
Crabp2
Fgf18
Pthr1
Vegfa
Day 1
Day 3
Day 8

Figure A2. Changes in gene expression with ketoconazole treatment.

PLM cultures established from the whole limb buds of wildtype mice and treated with ketoconazole (keto, 1µM) on day 0 exhibit similar changes in gene expression, evaluated by qPCR, as cultures established from *Cyp26b1*$^{-/-}$ mice. Error bars represent 1 s.d. Significance was evaluated in comparison to wildtype controls on the same day and is represented as follows: *P<0.05, **P<0.01, #P<0.001.

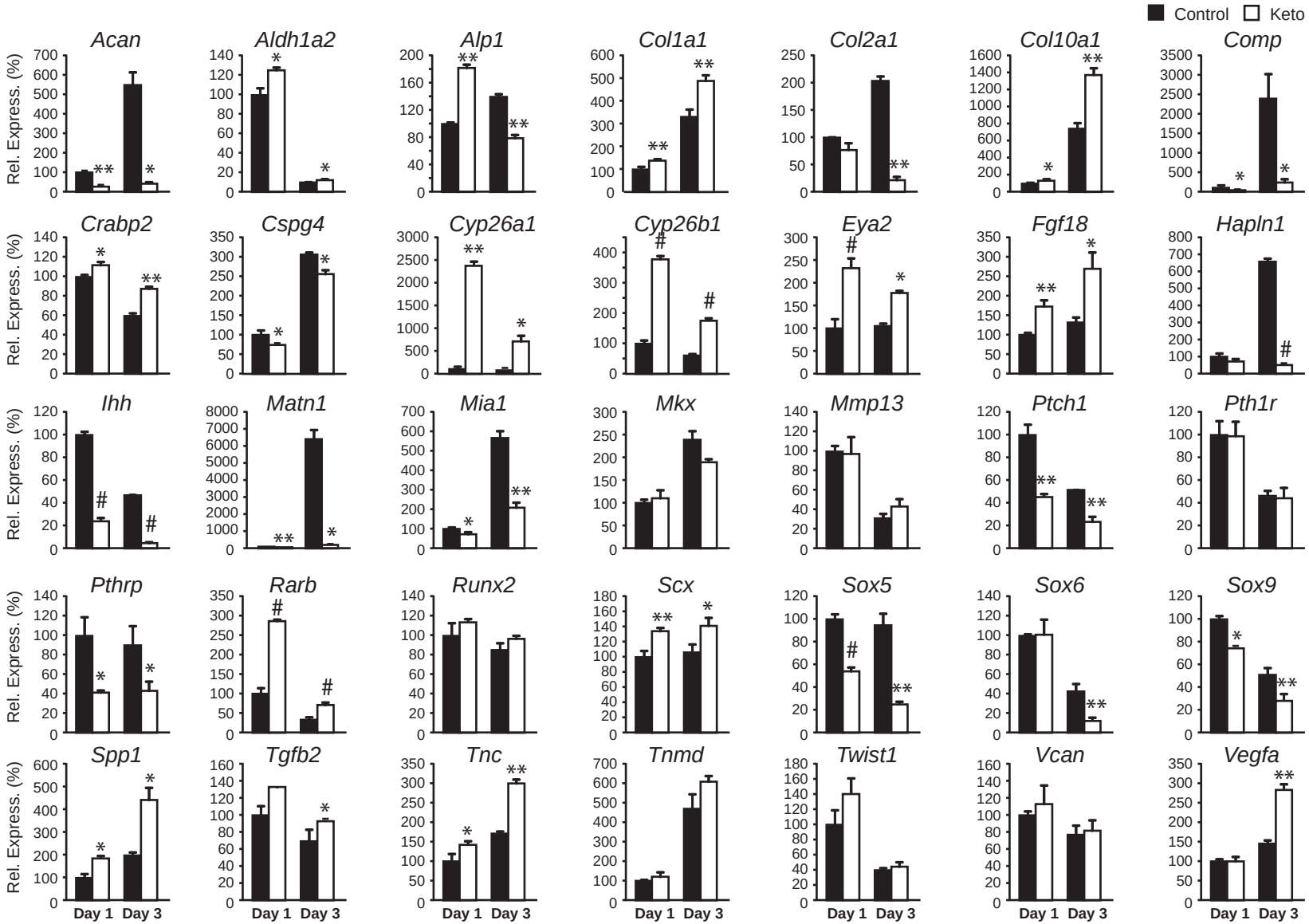
Control
Keto
Acan
Aldh1a2
Alp1
Col1a1
Col2a1
Col10a1
Comp
Crabp2
Cspg4
Cyp26a1
Cyp26b1
Eya2
Fgf18
Hapln1
Ihh
Matn1
Mia1
Mkx
Mmp13
Ptch1
Pth1r
Pthrp
Rarb
Runx2
Scx
Sox5
Sox6
Sox9
Spp1
Tgfb2
Tnc
Tnmd
Twist1
Vcan
Vegfa
Rel. Express. (%)
Day 1
Day 3

Figure A3. Ketoconazole and DEAB treatments.

A) Increasing doses of DEAB increases the activity of a Col2-LUC reporter and decreases the activity of a RARE-LUC reporter. Conversely, increasing doses of ketoconazole decreases the activity of a Col2-LUC reporter and increases the activity of a RARE-LUC reporter. Cells were treated with DEAB or ketoconzaole at the initiation of culture (day 0) and lysed for collection of luciferase extracts on day 2. B) Treatment of wildtype PLM cultures with ketoconazole (keto, 1µM) or DEAB (10µM) on day 0 or day 1 has similar effects on the chondrogenic program, as demonstrated by alcian blue staining of 4 and 8 day-old cultures. C) Treatment of wildtype PLM cultures established from proximal and distal regions of the limb with ketoconazole or DEAB on day 0 or day 1 has a similar effect on both Col2-LUC and RARE-LUC reporter activity. Reporter activity was measured after 3 days of culture. Scale bar, 2mm. Error bars represent 1 s.d. Significance was evaluated in comparison to wildtype controls of the same limb region (P or D) and is represented as follows: *$p<0.05$; **$p<0.01$; $^{\#}p<0.001$.

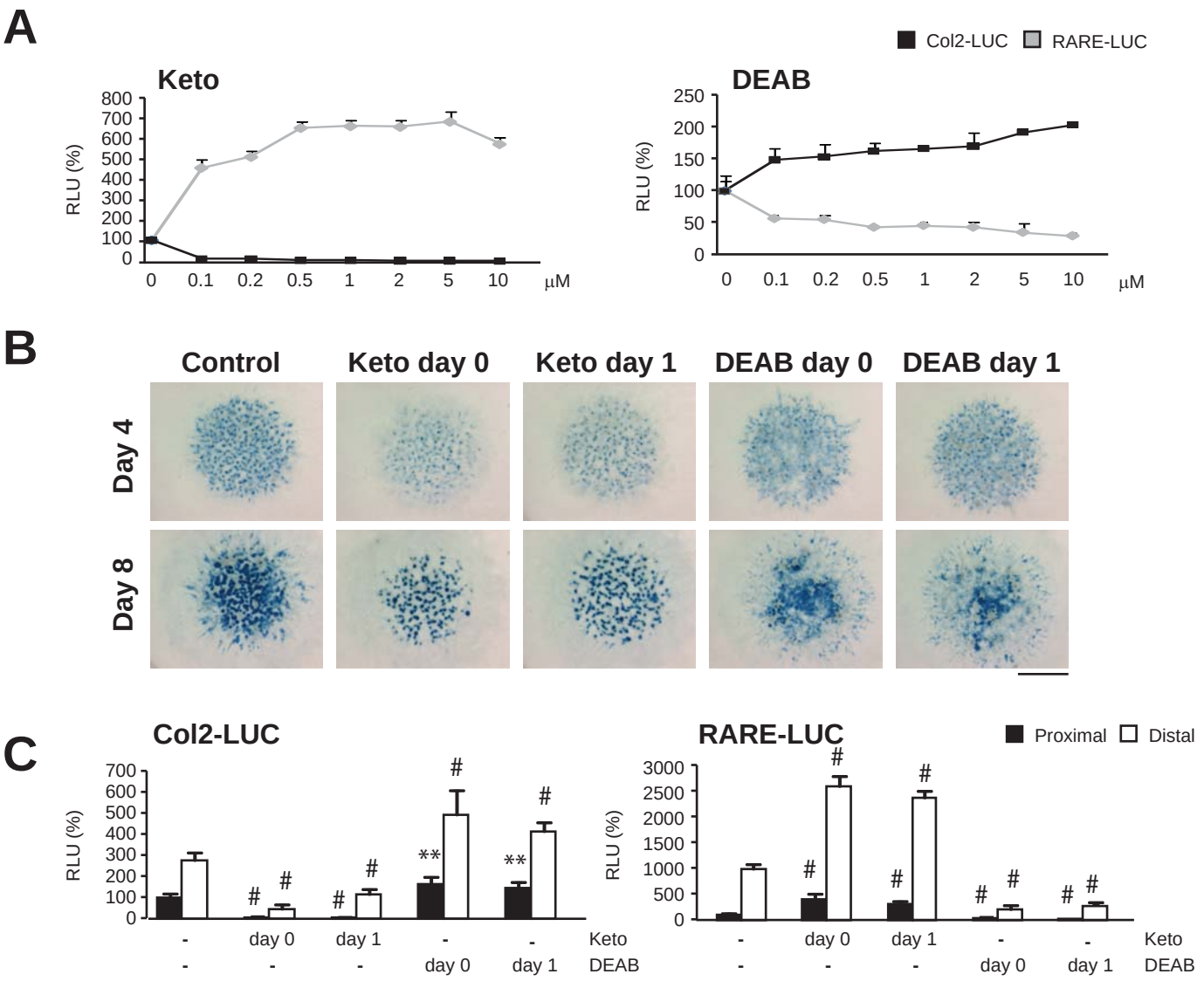
A
Col2-LUC
RARE-LUC
Keto
DEAB
RLU (%)
μM
B
Control
Keto day 0
Keto day 1
DEAB day 0
DEAB day 1
Day 4
Day 8
C
Col2-LUC
RARE-LUC
Proximal
Distal
RLU (%)
Keto
DEAB
day 0
day 1

Figure A4. Inhibition of chondrogenesis reflects an increase in tenogenesis.

A) qPCR analysis of tendon markers *Eya2*, *Mkx*, and *Tgfb2* in PLM cultures after 1 or 3 days of culture. B) *Rarb*, *Col1a1*, *Tnmd* expression were evaluated by qPCR in PLM cultures derived from proximal and distal limb regions of wildtype mice and treated with DEAB (10μM) or ketoconazole (keto, 1μM) for 1 or 3 days. C) Alcian blue staining of PLM cultures established from *ScxGFP*$^{+}$ mice treated with ketoconazole, DEAB, TGFb1 (Tb1, 2 ng/ml), and/or BMP4 (B4, 20 ng/ml) after 8 days of culture. Scale bar, 2mm. Error bars represent 1 s.d. Significance was evaluated in comparison to untreated controls of the same limb region on the same day and is represented as follows: *P<0.05, **P<0.01, #P<0.001.

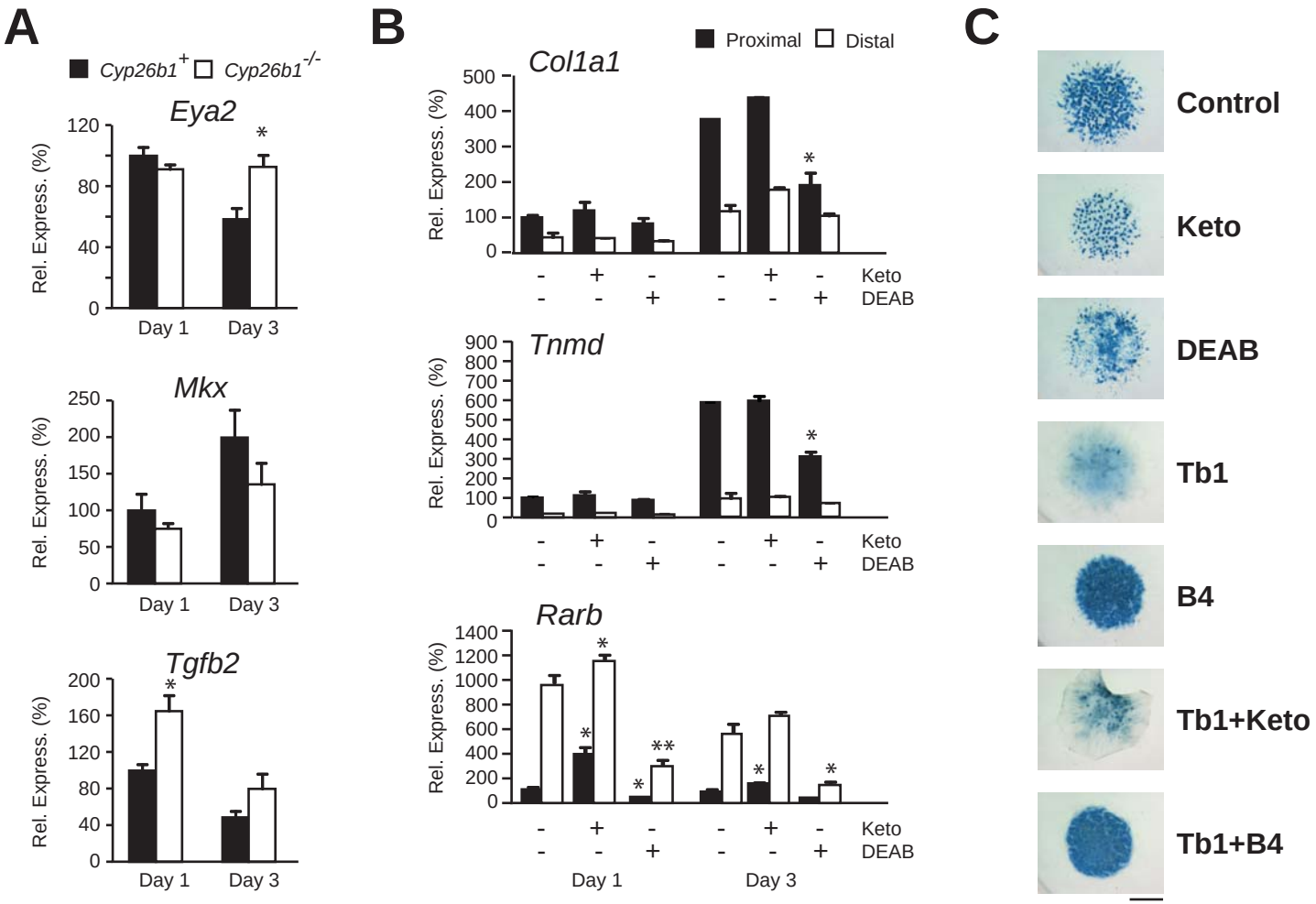
A
Cyp26b1+ Cyp26b1-/-
Eya2
Rel. Express. (%)
120
80
40
0
Day 1
Day 3
*
Mkx
250
200
150
100
50
0
Tgfb2
200
160
120
80
40
B
Proximal
Distal
Col1a1
500
400
300
200
100
- + - - + - Keto
- - + - - + DEAB
Tnmd
900
800
700
600
500
400
300
Rarb
1400
1200
1000
**
C
Control
Keto
DEAB
Tb1
B4
Tb1+Keto
Tb1+B4